

Science Advances



advances.science.org/cgi/content/full/3/4/e1600663/DC1

Supplementary Materials for **A dynamic hydrophobic core orchestrates allostery in protein kinases**

Jonggul Kim, Lalima G. Ahuja, Fa-An Chao, Youlin Xia, Christopher L. McClendon, Alexandr P. Kornev,
Susan S. Taylor, Gianluigi Veglia

Published 7 April 2017, *Sci. Adv.* **3**, e1600663 (2017)
DOI: 10.1126/sciadv.1600663

This PDF file includes:

- fig. S1. [^1H - ^{13}C] methyl-TROSY spectra of apo, nucleotide-bound (ATP γ C), and ternary (ATP γ N/PKI₅₋₂₄ and ATP γ N/PLN₁₋₁₉) forms of ^2H , ^{13}C -isoleucine, leucine, and valine (IVL)-labeled PKA-C.
- fig. S2. Plots of the IVL methyl group CSPs upon ligand binding.
- fig. S3. Mapping of the CSPs of the IVL methyl side-chain groups onto the crystal structure of PKA-C (PDB: 1ATP).
- fig. S4. Statistical analysis of the chemical shift changes.
- fig. S5. CHESCA (39) correlation matrix showing the degree of correlated chemical shift changes for the methyl side chains of IVL residues.
- fig. S6. Global conformational transitions mapped via linear CSPs probed by amide backbone resonances and methyl group resonances.
- fig. S7. Fast time scale (picosecond to nanosecond) conformational dynamics of the kinase upon ligand binding.
- fig. S8. Thermodynamics of ligand binding for PKA-C as measured by isothermal titration calorimetry (ITC).
- fig. S9. Slow time scale (microsecond to millisecond) conformational dynamics of the kinase.
- fig. S10. Slow time scale conformational dynamics of the kinase.
- fig. S11. Synchronous dynamics occurring in the highly conserved hydrophobic core.
- fig. S12. Location of I150 at the interface between different communities of PKA-C.
- fig. S13. Bridging residues connect the R-spine and C-spine at the PKA hydrophobic core.
- fig. S14. Western blot-based activity assay.

- fig. S15. Assembly of the R-spine for active protein kinases.
- fig. S16. Expression and purification of recombinant ^2H , ^{15}N , $^{13}\text{CH}_3$ -ILV, and PKA-C from *E. coli* bacteria.
- table S1. Classification of residues undergoing correlated chemical shift changes and their respective location in a specific community as identified by community map analysis.
- table S2. The dynamic light scattering data for three different forms of PKA-C.
- table S3. T_2 and S^2 values for methyl side-chain groups of apo PKA-C.
- table S4. T_2 and S^2 values for methyl side-chain groups of the ATP γ C-bound state of PKA-C.
- table S5. T_2 and S^2 values for methyl side-chain groups of the ATP γ N/PKI₅₋₂₄-bound state of PKA-C.
- table S6. Group fits of CPMG dispersion curves measured at 700 and 850 MHz of the apo form of PKA-C.
- table S7. Group fits of the CPMG relaxation dispersion curves measured at 700 and 850 MHz of the ATP γ C form of PKA-C.
- table S8. Single-quantum individual site fits of CPMG relaxation dispersion curves measured at 700 and 850 MHz of the apo form of PKA-C.
- table S9. Individual fits of the CPMG dispersion curves measured at 700 and 50 MHz of the ATP γ C-bound state of PKA-C.
- table S10. Single-quantum individual site fits of CPMG curves at 700 and 850 MHz of the ATP γ N/PKI₅₋₂₄-bound state of PKA-C.
- table S11. Approximate R_{ex} values from two points of the CPMG experiment for the ATP γ N/PLN₁₋₁₉-bound form of PKA-C.
- Reference (54)

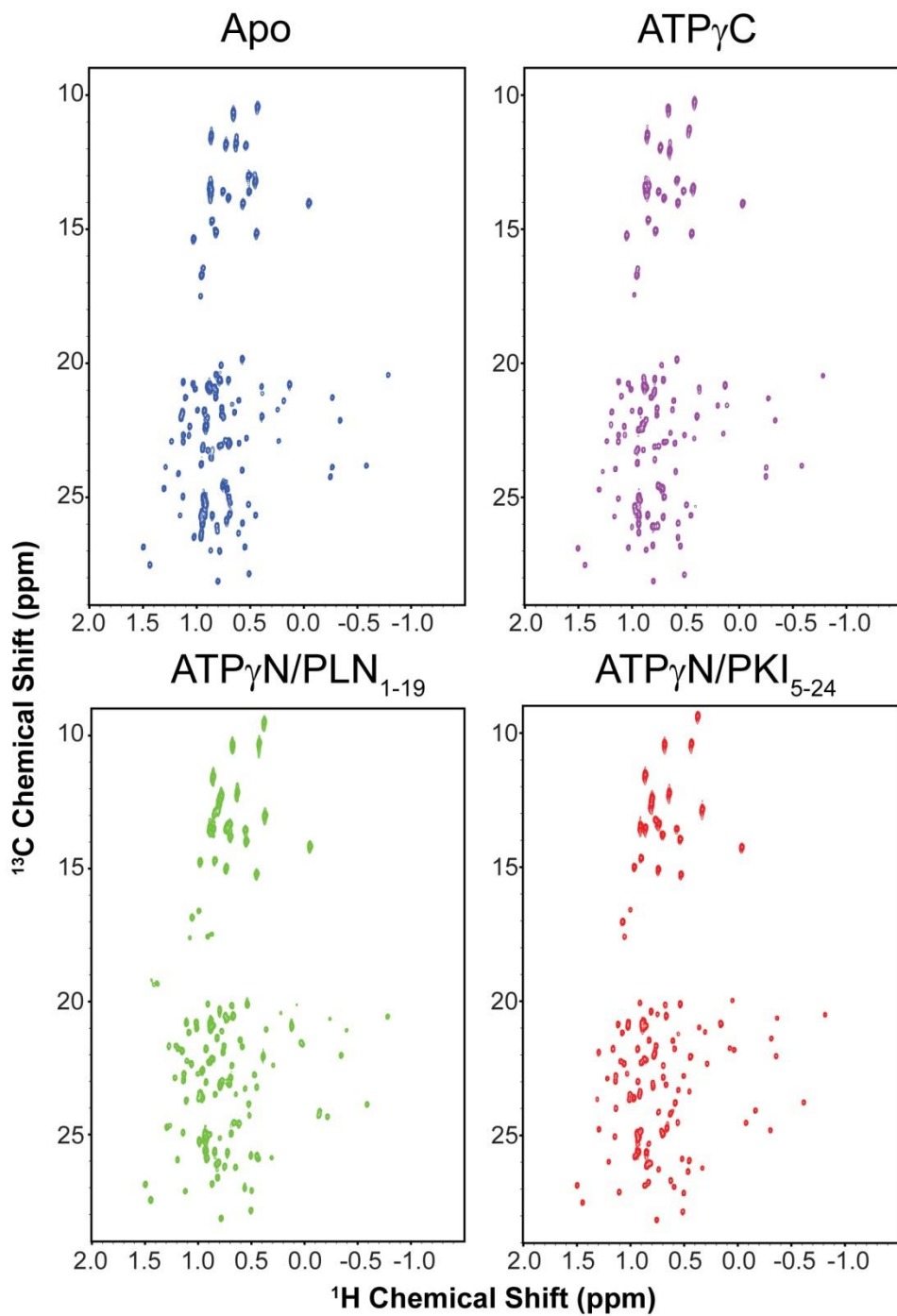


fig. S1. [^1H - ^{13}C] methyl-TROSY spectra of apo, nucleotide-bound (ATP} γ C), and ternary (ATP} γ N/PKI₅₋₂₄ and ATP} γ N/PLN₁₋₁₉) forms of ^2H , ^{13}C -isoleucine, leucine, and valine (IVL)-labeled PKA-C. Resonances assignments were performed on the ATP} γ N/PKI₅₋₂₄ bound form and transferred to the other forms following the chemical shift trajectories upon ligand titration experiments.

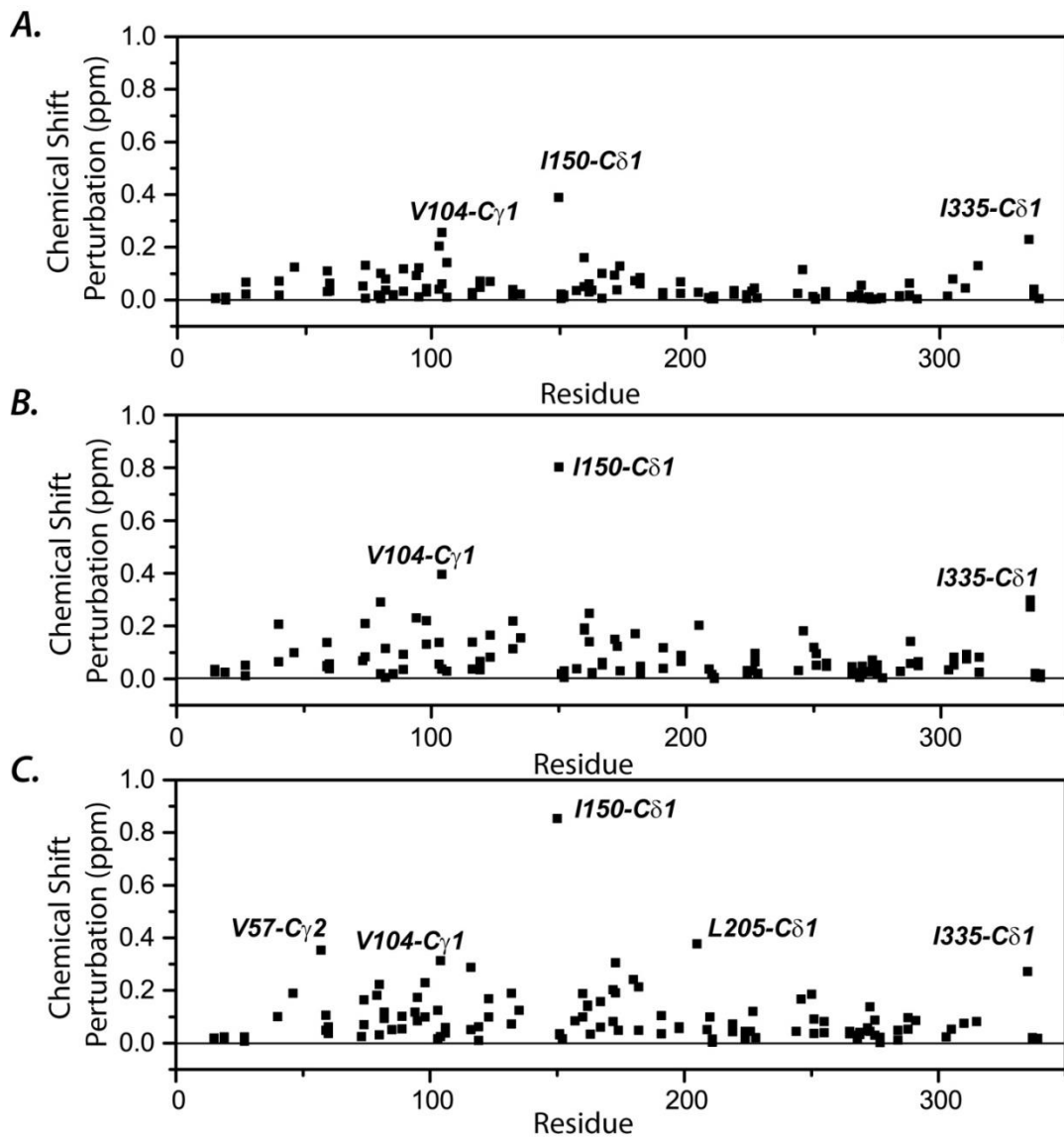


fig. S2. Plots of the IVL methyl group CSPs upon ligand binding. (A) CSPs upon ATP γ N binding to the apo PKA-C. (B) CSPs upon PLN₁₋₁₉ binding to ATP γ N saturated PKA-C. C. CSPs upon PKI5-24 binding to ATP γ N saturated PKA-C. Residues with large chemical shift changes belonging to the hydrophobic core are labeled in the graphs.

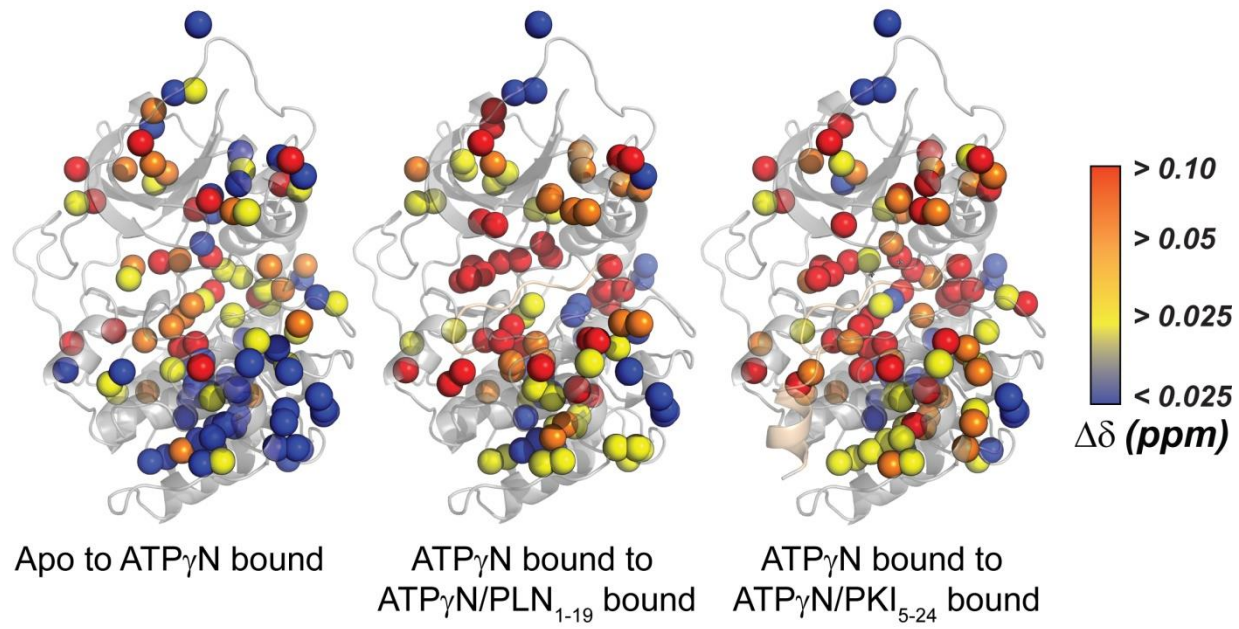


fig. S3. Mapping of the CSPs of the IVL methyl side-chain groups onto the crystal structure of PKA-C (PDB: 1ATP). Significant CSPs are present throughout the core upon nucleotide, substrate, and pseudo-substrate binding.

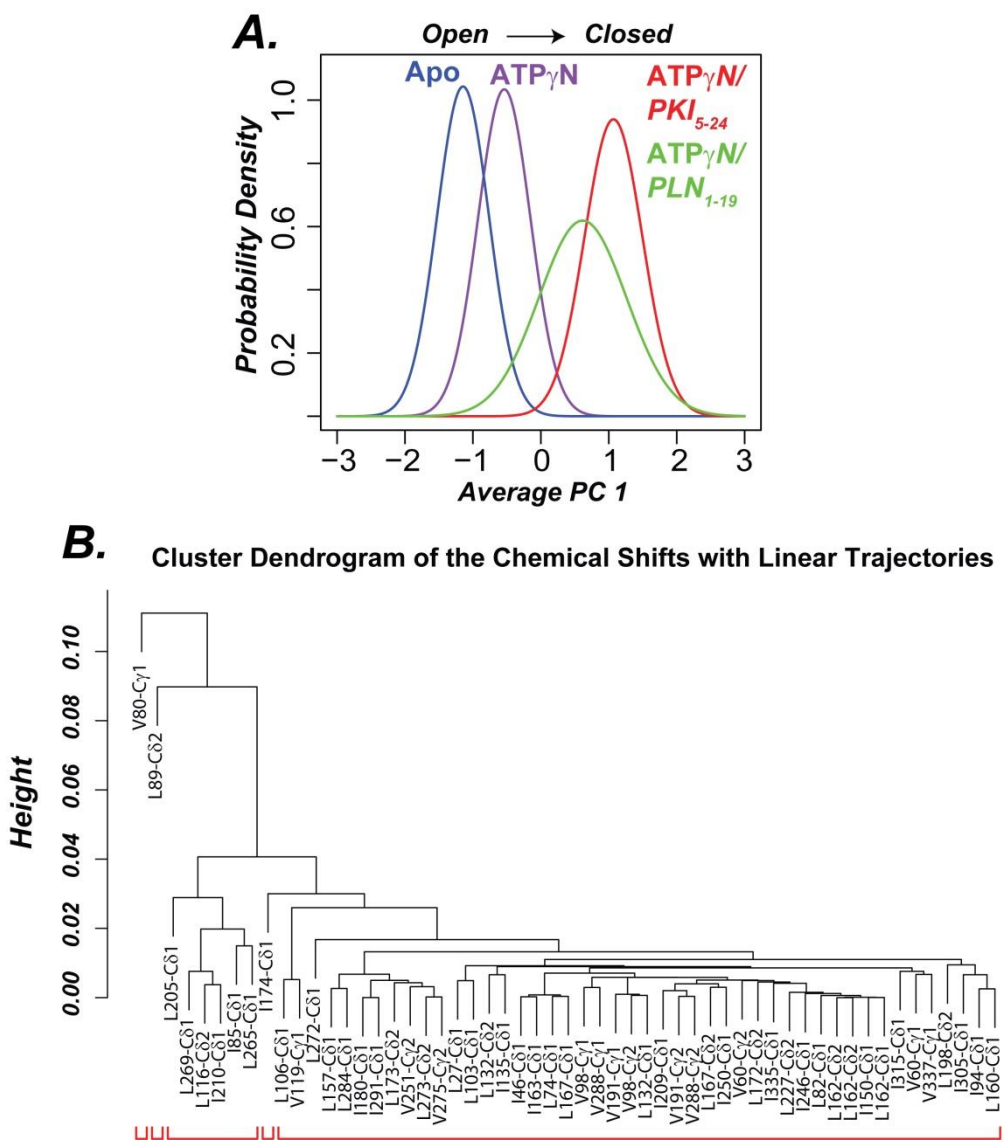


fig. S4. Statistical analysis of the chemical shift changes. (A) CONCISE (38) analysis: Plots of the probability density distributions versus the principal component 1 (PC1) of the chemical shift changes. The plot indicates the progression of all of the chemical shifts of the kinase from the open to the closed states. Dendrogram obtained from the CHESCA (39) analysis describing the clustering of methyl groups chemical shifts that move through correlated linear trajectories upon ligand binding. The majority of residues fall under a single group, showing that the majority of the residues of the enzyme transition between the open to the closed state.

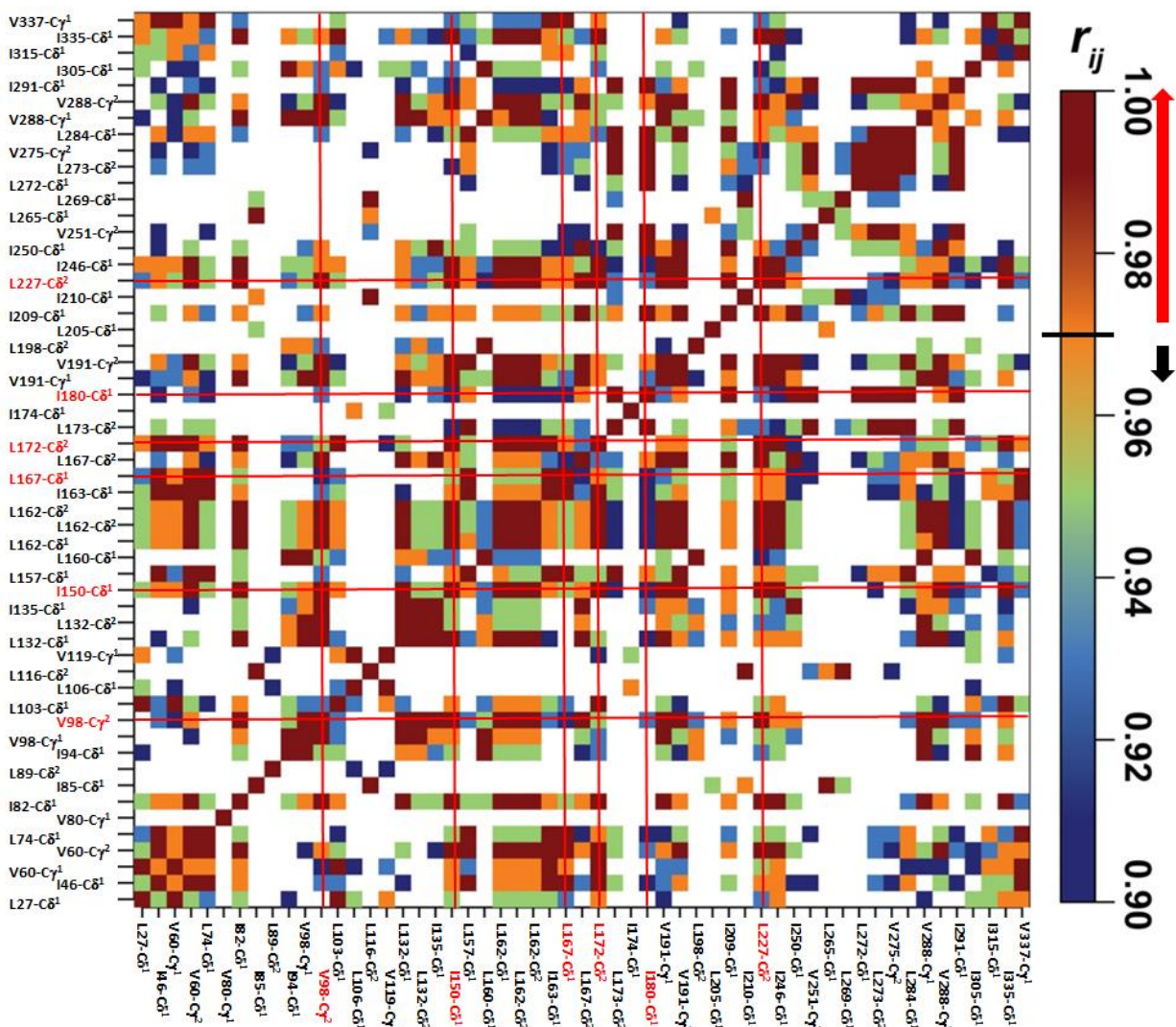


fig. S5. CHESCA (39) correlation matrix showing the degree of correlated chemical shift changes for the methyl side chains of IVL residues. The correlation coefficient, r_{ij} , indicates the degree correlated chemical shift changes along the linear trajectories.

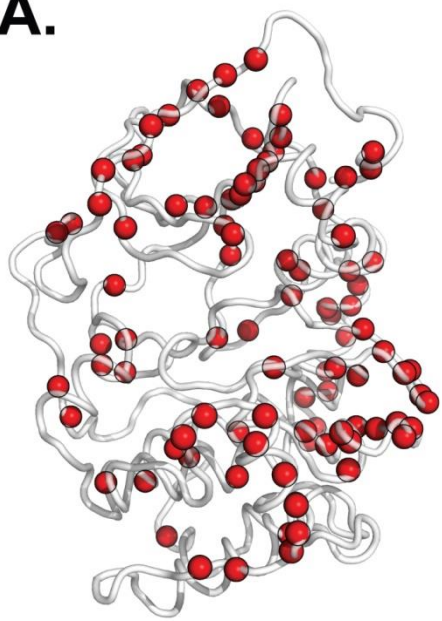
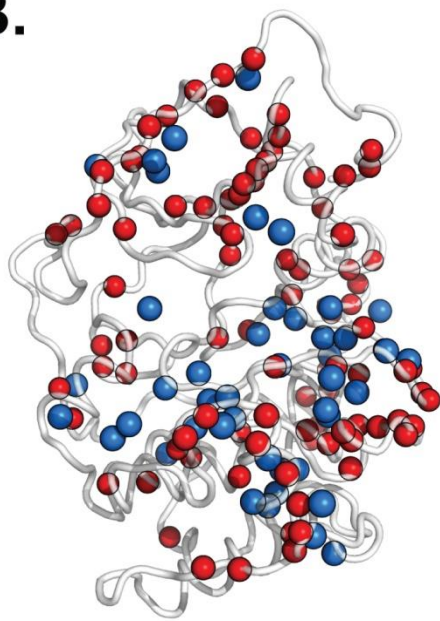
A.**B.**

fig. S6. Global conformational transitions mapped via linear CSPs probed by amide backbone resonances and methyl group resonances. (A) Backbone amide groups (red) that undergoing correlated linear chemical shift changes upon ligand binding (7). (B) Combined methyl (blue) side chain and backbone amide groups with correlated linear chemical shift changes upon ligand binding.

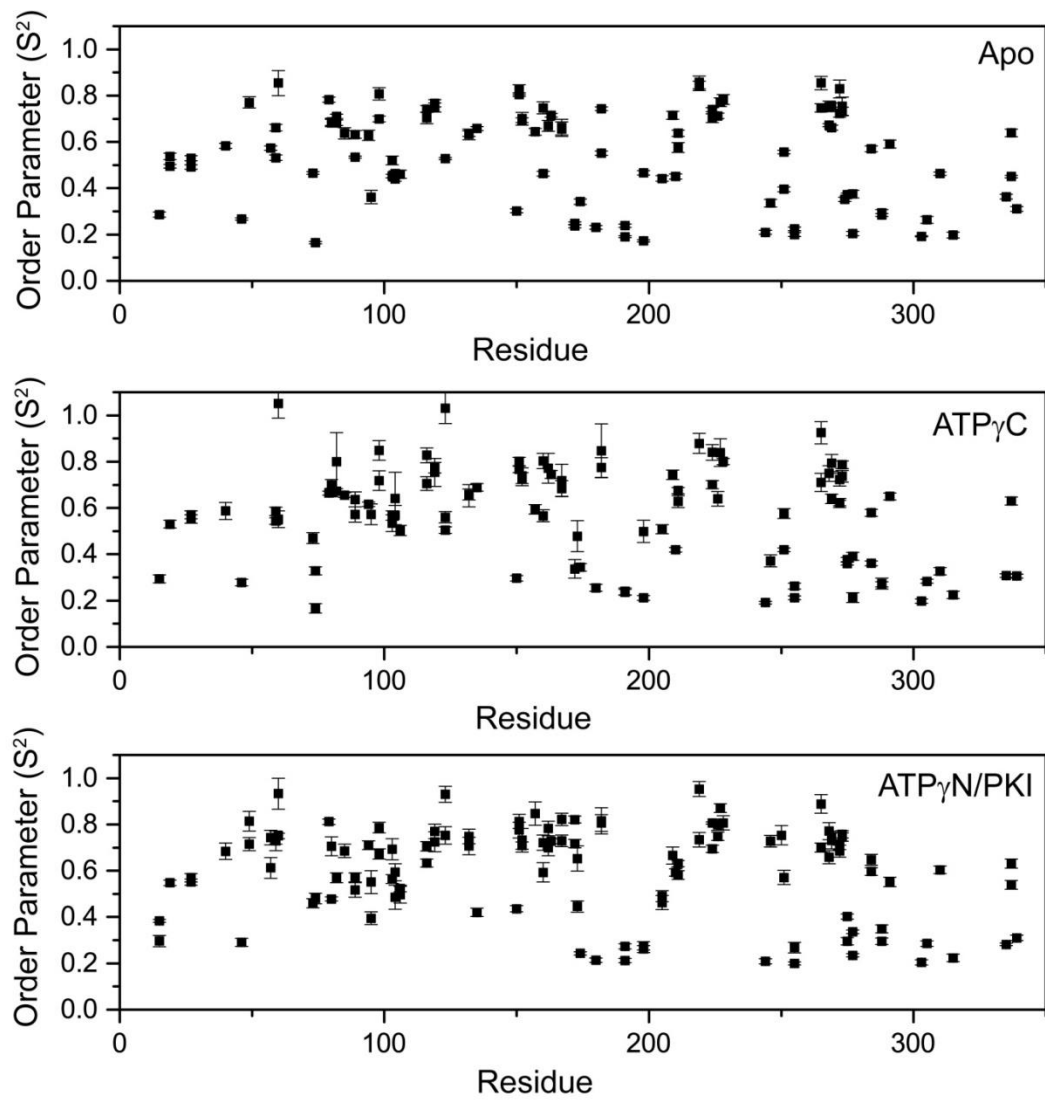


fig. S7. Fast time scale (picosecond to nanosecond) conformational dynamics of the kinase upon ligand binding. Plots of the methyl side-chain order parameters (S^2) for IVL residues calculated from ^2H relaxation experiments of the apo form, ATP γ C bound and ATP γ N/PKI₅₋₂₄ bound forms of PKA-C.

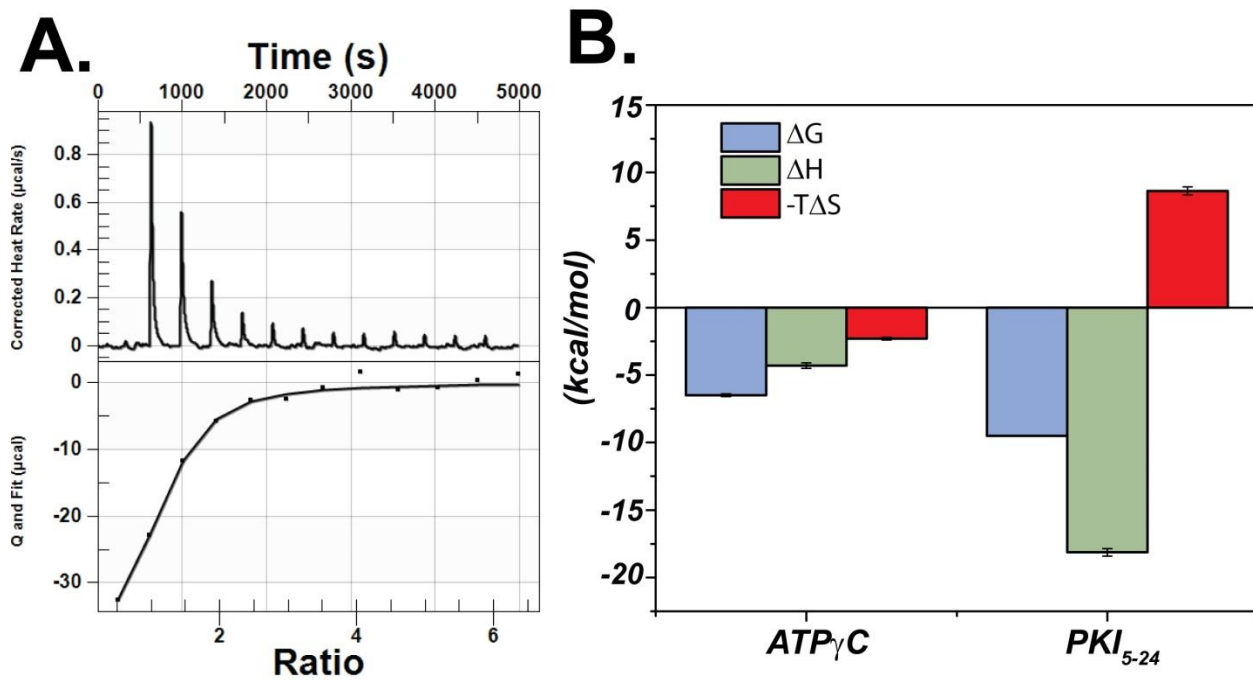


fig. S8. Thermodynamics of ligand binding for PKA-C as measured by isothermal titration calorimetry (ITC). (A) $ATP\gamma C$ binding titrations ($K_D = 17.6 \pm 3.0 \mu M$ and $\Delta H = -4.3 \pm 0.2$ kcal/mol). (B) Plot of the thermodynamic parameters for nucleotide and pseudo-substrate binding (19).

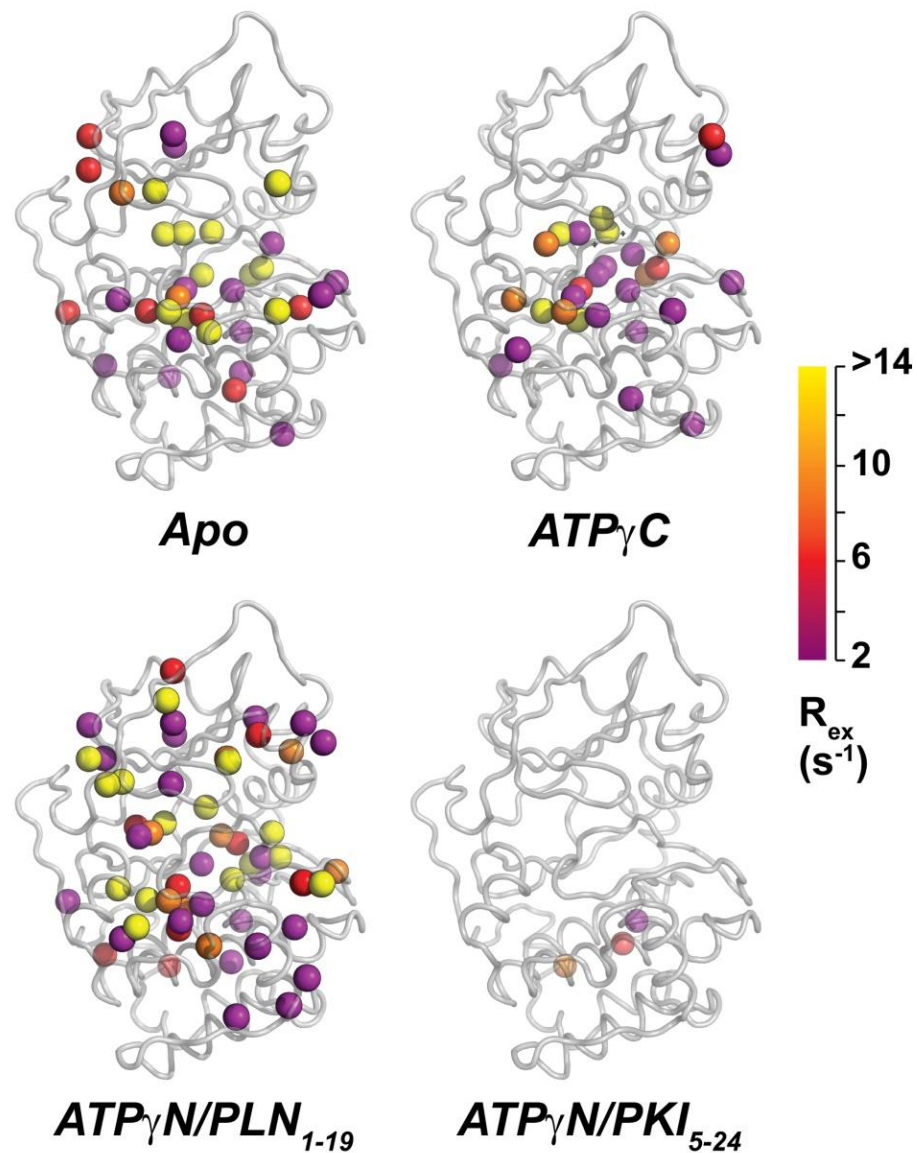


fig. S9. Slow time scale (microsecond to millisecond) conformational dynamics of the kinase. Residues exhibiting μ s-ms timescale dynamics as measured by ^{13}C SQ CPMG relaxation dispersion experiments (41) for the apo, nucleotide ($ATP\gamma C$), substrate ($ATP\gamma N/PLN_{1-19}$) and pseudo-substrate ($ATP\gamma N/PKI_{5-24}$) bound forms. For the $ATP\gamma N/PLN_{1-19}$ bound state of PKA-C, the approximate R_{ex} values were estimated using two points of the CPMG experiment to prevent changes occurring during the residual slow phosphorylation of the substrate during the length of the experiment (54).

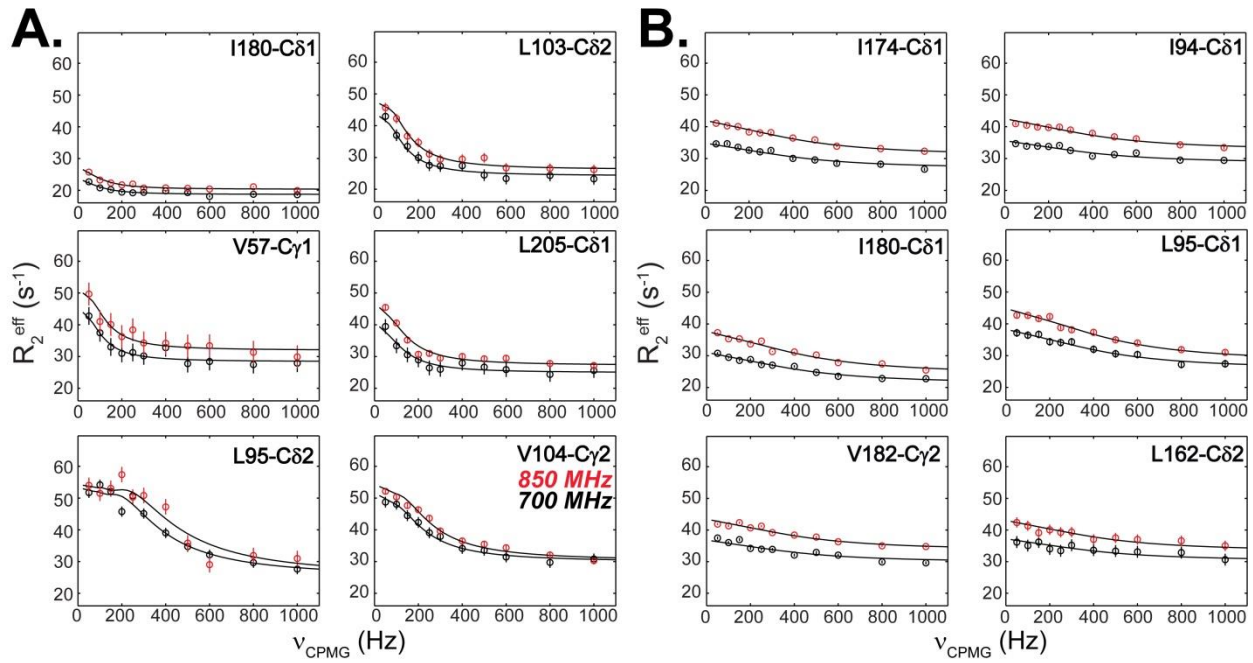


fig. S10. Slow time scale conformational dynamics of the kinase. Relaxation dispersion curves for residues exhibiting μ s-ms timescale dynamics as measured by ^{13}C SQ CPMG relaxation dispersion experiments (41) for the apo, nucleotide (ATP γ C), substrate (ATP γ N/PLN₁₋₁₉) and pseudo-substrate (ATP γ N/PKI₅₋₂₄) bound forms. For the ATP γ N/PLN₁₋₁₉ bound state of PKA-C, the approximate R_{ex} values were estimated using two points of the CPMG experiment to prevent the residual slow phosphorylation of the substrate during the length of the experiment (54).

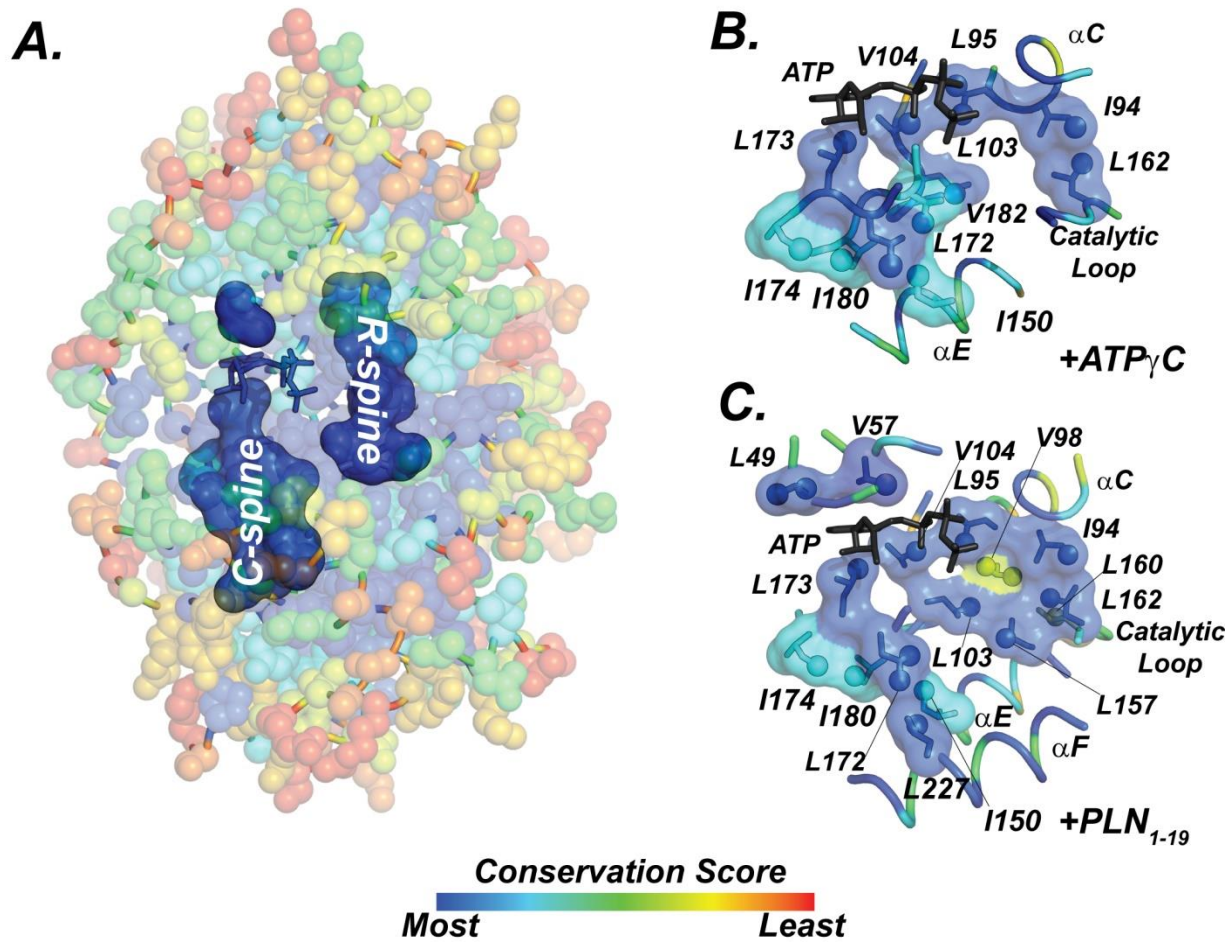


fig. S11. Synchronous dynamics occurring in the highly conserved hydrophobic core.
 (A) Conservation score for EPKs as imaged by Consurf (48) and mapped onto the structure of PKA-C. (B) Residues of the hydrophobic core with synchronous conformational dynamics in the nucleotide-bound state (ATP γ C). (C) Residues of the hydrophobic core experiencing significant conformational exchange in the substrate bound state (ATP γ N/PLN₁₋₁₉).

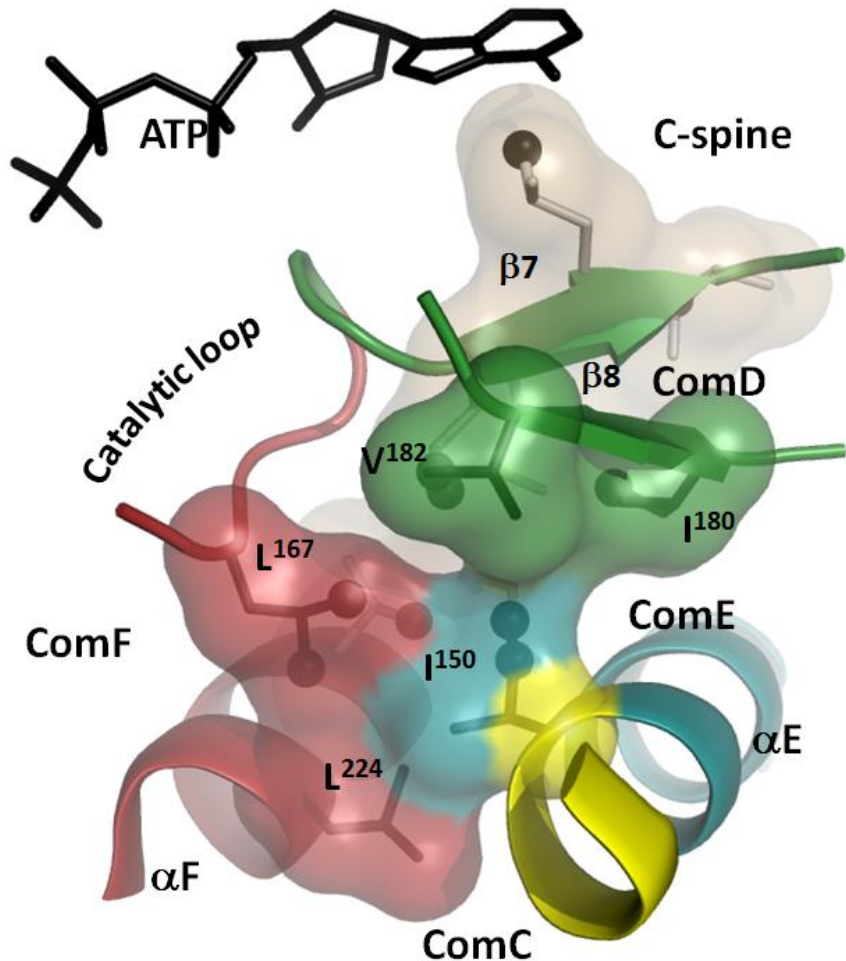


fig. S12. Location of I150 at the interface between different communities of PKA-C.

(A) I150 neighbors the catalytic and activation loop through L167, I180, and V182. With L224, these two residues directly connect the α E and α F helices with a highly conserved architecture (23). Previous community map analysis from MD trajectories (14) show that I150 is positioned at the interface between four different communities, integrating the motions between major structural elements of the kinase core (14).

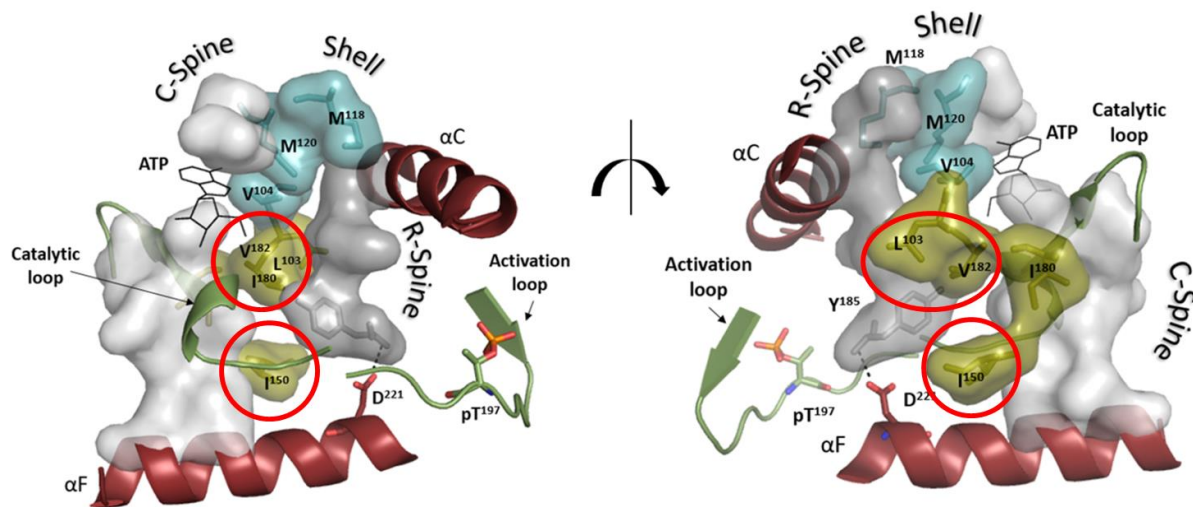


fig. S13. Bridging residues connect the R-spine and C-spine at the PKA hydrophobic core.
 Shell residues (teal) V104, M118 and M120 connect the R- and C-spines in the N-lobe of the kinase. Three residues V182, L203 and I180 (gold) connect the two spines in the center of the core. I150 (gold) connects the spines at the base closer to the α F Helix.

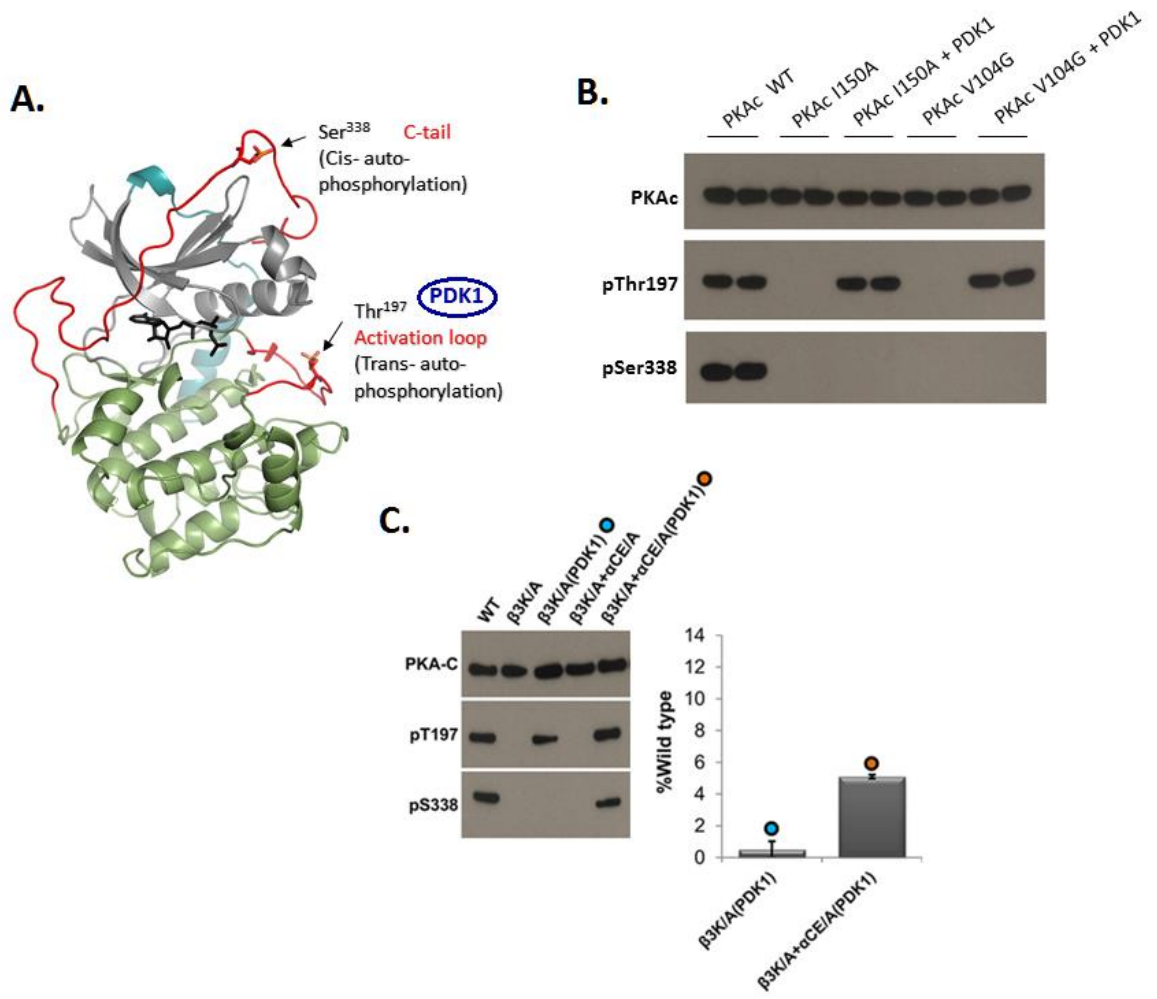


fig. S14. Western blot–based activity assay. (A) Phosphorylation of Thr197 and S338 render the kinase in an active state. Phosphorylation of Thr197 in the activation loop in vitro can be carried out in *trans* by either another active PKA-C or the upstream kinase PDK1, creating a salt bridge with H87 that anchors the C helix and completes the R-spine. Phosphorylation at Thr197 is essential for full activity. Phosphorylation on S338 occurs co-translationally in a *cis* fashion as part of the maturation cycle of PKA-C. It stabilizes the core and is essential for the regulated maturation of the C-subunit. (B) Western blot analysis of the V104G and I150A mutants for Thr197 and Ser338 phosphorylation. When expressed on their own both mutants are incapable of either Thr197 or Ser 338 phosphorylation. Phosphorylation of Thr197 is induced by co-expression of PDK1. The lack of Ser338 phosphorylation in the presence of Thr197 phosphorylation demonstrates that these mutants are essentially inactive. (C) Control experiments using previously characterized PKA mutants (54). Mutants that are unable to do Ser 338 despite PDK1 phosphorylation of Thr197 are seen to be catalytically dead. For even 5% of wild-type PKA-C activity, mutant must show a consistent phosphorylation of the *cis* Ser 338 site. (adapted from reference 54).

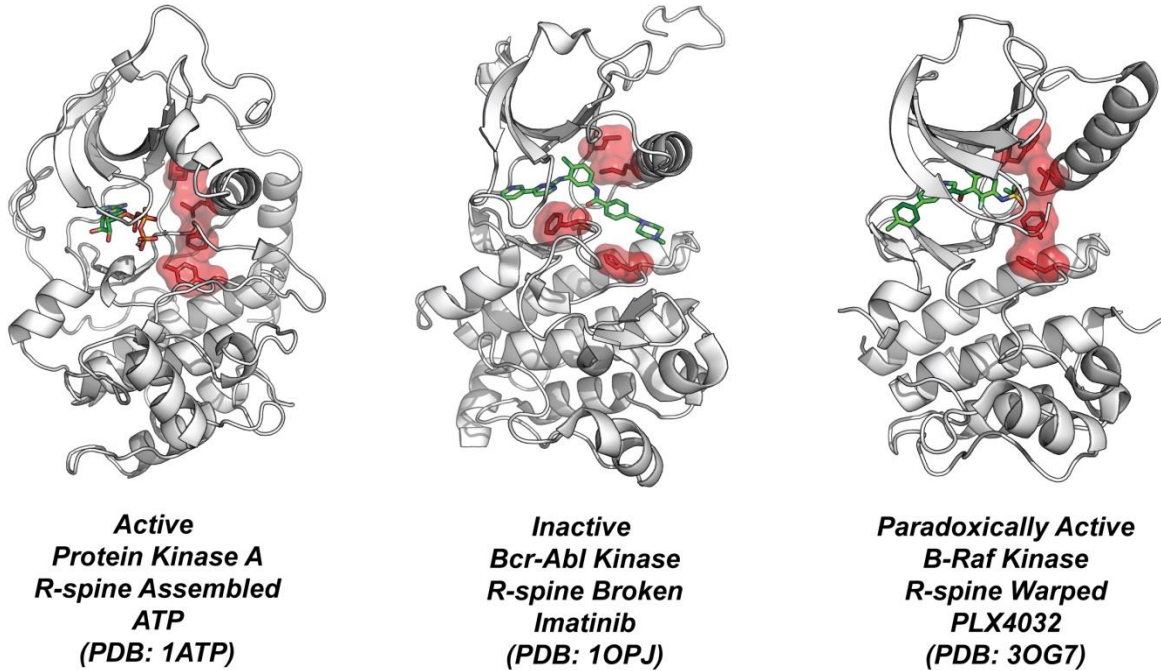


fig. S15. Assembly of the R-spine for active protein kinases. In PKA-C the R-spine is constitutively assembled by T197 phosphorylation and competent for catalysis with ATP. The specific kinase inhibitor imatinib selects the DFG out state, breaking the R-spine and inactivating the kinase. The specific B-Raf inhibitor, PLX4032, inhibits catalytic activity, but wraps the R-spine, creating a RAF dimer and induces signaling as a pseudo-kinase.

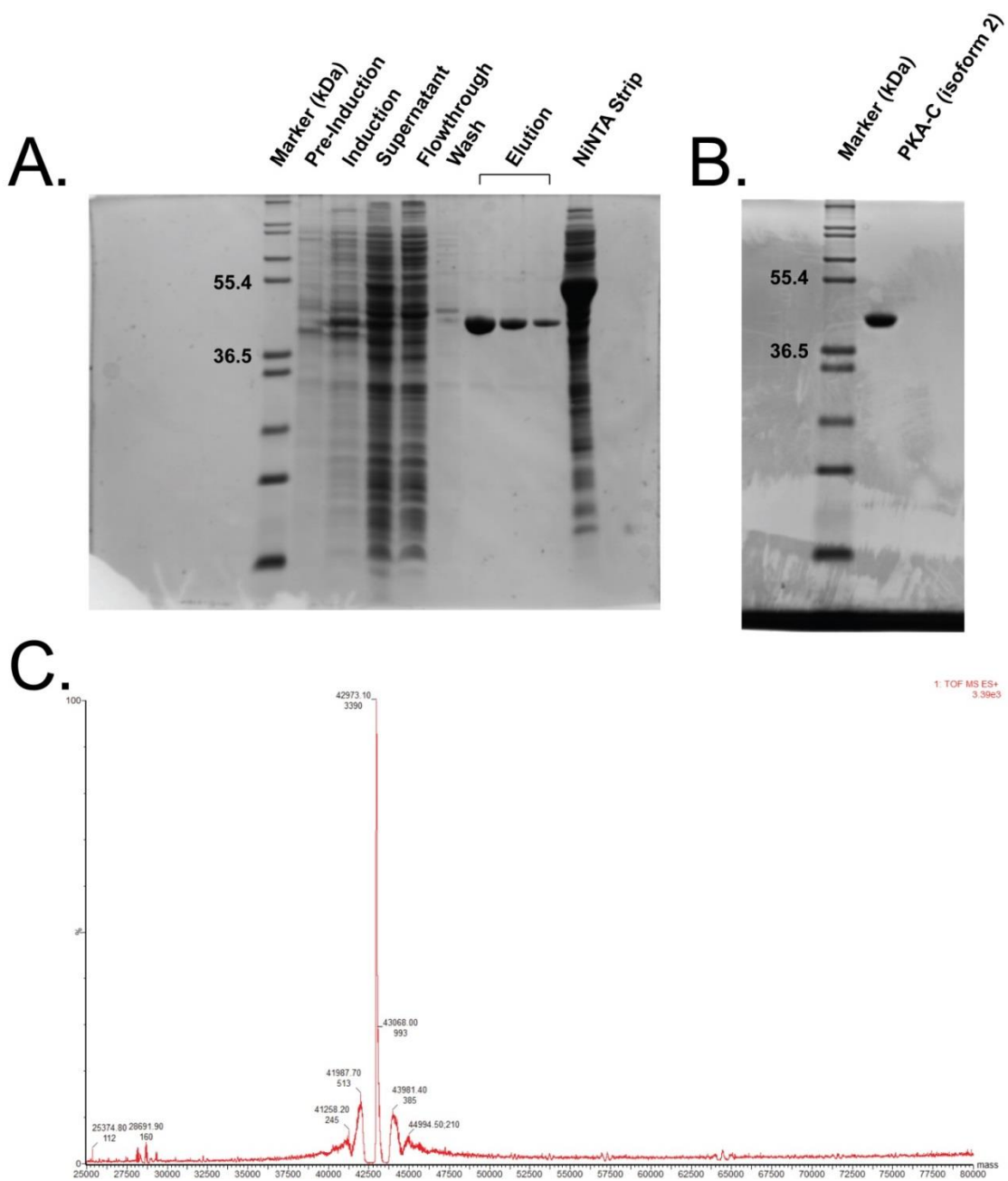


fig. S16. Expression and purification of recombinant ^2H , ^{15}N , $^{13}\text{CH}_3$ -ILV, and PKA-C from *E. coli* bacteria. (A) SDS-PAGE gel showing the overexpression of PKA-C and affinity chromatography using His₆-RII α (R213K). **(B)** SDS-PAGE gel showing the purity of isoform 2 of PKA-C after FPLC with a HiTrap SP column. **(C)** Mass spec data of ^2H , ^{15}N , $^{13}\text{CH}_3$ -ILV, PKA-C with >95% incorporation of ^2H on non-exchangable protons (excluding methyl labeling).

table S1. Classification of residues undergoing correlated chemical shift changes and their respective location in a specific community as identified by community map analysis.

Backbone resonances that have correlated shifts with ligand binding were reported previously (7).

Residue	Backbone	Side-Chain	Secondary Structure	Residue	Backbone	Side-Chain	Secondary Structure
L27-C δ 1	Com C	Com C	α A	L173-C δ 2	Com D	Com D	β 7
I46-C δ 1	Com A	Com A	β 1	I174-C δ 1	Com D	Com D	β 7
V60-C γ 1	Com A	Com A	β 2	I180-C δ 1	Com D	Com D	β 8
V60-C γ 2	Com A	Com A	β 2	V191-C γ 1	Com F	Com F	Mg ⁺²
L74-C δ 1	Com B	Com B	β 3	V191-C γ 2	Com F	Com F	Mg ⁺²
V80-C γ 1	Com B	Com B	α B	L198-C δ 2	Com F	Com F	P+1
L82-C δ 1	Com B	Com B	α B	L205-C δ 1	Com F	Com F	P+1
I85-C δ 1	Com B	Com B	α C	I209-C δ 1	Com F	Com F	P+1
L89-C δ 2	Com C	Com B	α C	I210-C δ 1	Com F	Com F	P+1
I94-C δ 1	Com C	Com C	α C	V219-C γ 2	Com F	Com F	α F
V98-C γ 1	Com C	Com C	α C	L227-C δ 2	Com F	Com F	α F
V98-C γ 2	Com C	Com C	α C	I246-C δ 1	Com G	Com G	α G
L103-C δ 1	Com C	Com C	α C	I250-C δ 1	Com G	Com G	α G
L106-C δ 1	Com C	Com C	α C- β 4	V251-C γ 2	Com G	Com G	α G
L116-C δ 2	Com B	Com B	β 4	L265-C δ 1	Com H	Com H	α H
V119-C γ 1	Com A	Com A	β 4	L269-C δ 1	Com F	Com F1	α H
L132-C δ 1	Com D	Com D	α D	L272-C δ 1	Com F	Com F	α H
L132-C δ 2	Com D	Com D	α D	L273-C δ 2	Com F	Com F	α H
I135-C δ 1	Com D	Com D	α D	V275-C γ 2	Com F	Com F	α H- α I
I150-C δ 1	Com C	Com E	α E	L284-C δ 1	Com H	Com F	α H- α I
L157-C δ 1	Com C	Com C	α E	V288-C γ 1	Com H	Com C	α I
L160-C δ 1	Com C	Com C	α E- β 6	V288-C γ 2	Com H	Com C	α I
L162-C δ 1	Com C	Com C	β 6	I291-C δ 1	Com H	Com H	α I
I163-C δ 1	Com C	Com F	β 6	I305-C δ 1	Com E	Com E	α J
L167-C δ 1	Com F	Com F	β 6- β 7	I315-C δ 1	Com D	Com D	C-tail
L167-C δ 2	Com F	Com F	β 6- β 7	I335-C δ 1	Com B	Com A	C-tail
L172-C δ 1	Com D	Com D	β 7	V337-C γ 1	Com B	Com B	C-tail
L172-C δ 2	Com D	Com D	β 7				

table S2. The dynamic light scattering data for three different forms of PKA-C. The global rotational correlation times (31, 29, and 28 ns for apo binary and ternary forms, respectively) were determined by the average values of hydrodynamic radii using the Stokes-Einstein equation.

Record	Sample Name	T (°C)	Z-Ave (r.nm)	PdI	Pk 1 Mean Size (r.nm)	Pk 2 Mean Size (r.nm)	Pk 3 Mean Size (r.nm)
1	apo_PKA_250uM	25	3.287	0.036	3.385	0	0
2	apo_PKA_250uM	25	3.284	0.069	3.381	0	0
3	apo_PKA_250uM	25	3.256	0.026	3.333	0	0
4	apo_PKA_250uM	25	3.245	0.042	3.356	0	0
5	apo_PKA_250uM	25	3.24	0.05	3.353	0	0
6	apo_PKA_250uM	25	3.226	0.05	3.331	0	0
1	binary_PKA_230uM	25	3.192	0.072	3.345	0	0
2	binary_PKA_230uM	25	3.195	0.091	3.256	0	0
3	binary_PKA_230uM	25	3.232	0.098	3.256	0	0
4	binary_PKA_230uM	25	3.222	0.13	3.165	0	0
5	binary_PKA_230uM	25	3.141	0.069	3.243	0	0
6	binary_PKA_230uM	25	3.174	0.051	3.317	0	0
1	closed_PKA_200uM	25	3.114	0.103	3.14	0	0
2	closed_PKA_200uM	25	3.104	0.079	3.168	0	0
3	closed_PKA_200uM	25	3.13	0.102	3.177	0	0
4	closed_PKA_200uM	25	3.161	0.135	3.171	1772	0
5	closed_PKA_200uM	25	3.148	0.119	3.171	2279	0
6	closed_PKA_200uM	25	3.133	0.106	3.221	0	0

table S3. T_2 and S^2 values for methyl side-chain groups of apo PKA-C.

Residue	T_2 (ms)	S^2	Residue	T_2 (ms)	S^2
V15-C γ 1	8.19 ± 0.31	0.29 ± 0.01	I174-C δ 1	6.86 ± 0.24	0.34 ± 0.01
L19-C δ 1	4.36 ± 0.11	0.54 ± 0.01	I180-C δ 1	10.15 ± 0.35	0.23 ± 0.01
L19-C δ 2	4.74 ± 0.08	0.49 ± 0.01	V182-C γ 1	3.15 ± 0.03	0.74 ± 0.01
L27-C δ 1	4.77 ± 0.09	0.49 ± 0.01	V182-C γ 2	4.25 ± 0.08	0.55 ± 0.01
L27-C δ 2	4.42 ± 0.09	0.53 ± 0.01	V191-C γ 1	12.30 ± 0.23	0.19 ± 0.00
L40-C δ 2	4.02 ± 0.08	0.58 ± 0.01	V191-C γ 2	9.82 ± 0.29	0.24 ± 0.01
I46-C δ 1	8.80 ± 0.15	0.27 ± 0.00	L198-C δ 1	5.02 ± 0.11	0.47 ± 0.01
L49-C δ 1	3.04 ± 0.10	0.78 ± 0.02	L198-C δ 2	13.56 ± 0.42	0.17 ± 0.01
V57-C γ 1	4.09 ± 0.07	0.29 ± 0.01	L205-C δ 1	5.30 ± 0.15	0.44 ± 0.01
L59-C δ 1	4.02 ± 0.09	0.53 ± 0.01	I209-C δ 1	3.28 ± 0.08	0.72 ± 0.02
L59-C δ 2	3.54 ± 0.07	0.66 ± 0.01	I210-C δ 1	5.19 ± 0.13	0.45 ± 0.01
V60-C γ 1	2.74 ± 0.17	0.85 ± 0.05	L211-C δ 1	4.07 ± 0.15	0.58 ± 0.02
I73-C δ 1	5.03 ± 0.06	0.47 ± 0.01	L211-C δ 2	3.68 ± 0.48	0.64 ± 0.01
L74-C δ 2	14.24 ± 0.39	0.16 ± 0.00	V219-C γ 1	2.73 ± 0.09	0.86 ± 0.03
V79-C γ 1	2.99 ± 0.04	0.78 ± 0.01	V219-C γ 2	2.78 ± 0.07	0.84 ± 0.02
V80-C γ 1	3.41 ± 0.08	0.68 ± 0.02	L224-C δ 1	3.17 ± 0.04	0.74 ± 0.01
V80-C γ 2	3.44 ± 0.08	0.68 ± 0.02	L224-C δ 2	3.34 ± 0.09	0.70 ± 0.02
L82-C δ 1	3.30 ± 0.04	0.71 ± 0.01	V226-C γ 2	3.29 ± 0.05	0.71 ± 0.01
L82-C δ 2	3.43 ± 0.06	0.68 ± 0.01	L227-C δ 2	3.04 ± 0.07	0.77 ± 0.02
I85-C δ 1	3.78 ± 0.14	0.64 ± 0.02	I228-C δ 1	2.99 ± 0.08	0.78 ± 0.02
L89-C δ 1	3.71 ± 0.10	0.63 ± 0.02	I244-C δ 1	11.19 ± 0.46	0.21 ± 0.01
L89-C δ 2	4.39 ± 0.04	0.53 ± 0.01	I246-C δ 1	6.98 ± 0.33	0.34 ± 0.02
I94-C δ 1	3.73 ± 0.13	0.63 ± 0.02	V251-C γ 1	5.93 ± 0.16	0.40 ± 0.01
L95-C δ 2	6.48 ± 0.52	0.36 ± 0.03	V251-C γ 2	4.22 ± 0.06	0.56 ± 0.01
L89-C δ 2	5.03 ± 0.06	0.47 ± 0.01	V255-C γ 1	10.43 ± 0.36	0.22 ± 0.01
V98-C γ 1	3.36 ± 0.06	0.70 ± 0.02	V255-C γ 2	11.72 ± 0.49	0.20 ± 0.01
V98-C γ 2	2.90 ± 0.09	0.81 ± 0.02	L265-C δ 1	2.74 ± 0.09	0.85 ± 0.03
L103-C δ 1	4.50 ± 0.16	0.52 ± 0.02	L265-C δ 2	3.14 ± 0.07	0.75 ± 0.02
L103-C δ 2	5.18 ± 0.09	0.45 ± 0.02	L268-C δ 1	3.84 ± 0.03	0.67 ± 0.01
V104-C γ 1	5.33 ± 0.11	0.44 ± 0.01	L268-C δ 2	3.11 ± 0.09	0.75 ± 0.02
V104-C γ 2	5.06 ± 0.13	0.46 ± 0.01	L269-C δ 1	3.11 ± 0.05	0.75 ± 0.01
L106-C δ 1	5.09 ± 0.20	0.46 ± 0.02	L269-C δ 2	3.54 ± 0.06	0.66 ± 0.01
L116-C δ 1	3.33 ± 0.12	0.70 ± 0.02	L272-C δ 1	2.83 ± 0.13	0.83 ± 0.03
L116-C δ 2	3.16 ± 0.06	0.74 ± 0.01	L272-C δ 2	3.24 ± 0.07	0.72 ± 0.02
V119-C γ 1	3.06 ± 0.06	0.77 ± 0.02	L273-C δ 1	3.20 ± 0.08	0.73 ± 0.02
V119-C γ 2	3.13 ± 0.08	0.75 ± 0.02	L273-C δ 2	3.11 ± 0.16	0.75 ± 0.04
V123-C γ 2	4.44 ± 0.04	0.53 ± 0.00	V275-C γ 1	6.29 ± 0.09	0.37 ± 0.01
L132-C δ 1	3.70 ± 0.14	0.63 ± 0.02	V275-C γ 2	6.66 ± 0.17	0.35 ± 0.01
L132-C δ 2	3.68 ± 0.07	0.63 ± 0.01	L277-C δ 1	11.44 ± 0.52	0.20 ± 0.01

I135-C δ 1	3.56 ± 0.05	0.66 ± 0.01	L277-C δ 2	6.25 ± 0.28	0.38 ± 0.02
I150-C δ 1	7.56 ± 0.22	0.30 ± 0.01	L284-C δ 1	4.11 ± 0.09	0.57 ± 0.01
V151-C γ 1	2.91 ± 0.03	0.80 ± 0.01	V288-C γ 1	8.26 ± 0.18	0.28 ± 0.02
V151-C γ 2	2.84 ± 0.07	0.83 ± 0.02	V288-C γ 2	7.99 ± 0.42	0.29 ± 0.01
L152-C δ 1	3.38 ± 0.05	0.69 ± 0.01	I291-C δ 1	3.97 ± 0.12	0.59 ± 0.02
L152-C δ 2	3.35 ± 0.13	0.70 ± 0.03	I303-C δ 1	12.18 ± 0.18	0.19 ± 0.00
L157-C δ 1	3.64 ± 0.08	0.64 ± 0.01	I305-C δ 1	8.90 ± 0.50	0.26 ± 0.01
L160-C δ 1	3.14 ± 0.11	0.75 ± 0.03	V310-C γ 1	5.06 ± 0.07	0.46 ± 0.01
L160-C δ 2	5.06 ± 0.12	0.46 ± 0.01	I315-C δ 1	11.84 ± 0.76	0.20 ± 0.01
L162-C δ 2	3.50 ± 0.12	0.67 ± 0.02	I335-C δ 1	6.45 ± 0.76	0.36 ± 0.01
I163-C δ 1	3.28 ± 0.03	0.71 ± 0.01	V337-C γ 1	3.67 ± 0.09	0.64 ± 0.02
L167-C δ 1	3.58 ± 0.17	0.66 ± 0.03	V337-C γ 2	5.20 ± 0.07	0.45 ± 0.01
L167-C δ 2	3.53 ± 0.18	0.66 ± 0.03	I339-C δ 1	7.55 ± 0.24	0.31 ± 0.01
L172-C δ 1	9.90 ± 0.30	0.24 ± 0.01			
L172-C δ 2	9.43 ± 0.23	0.25 ± 0.01			

table S4. T_2 and S^2 values for methyl side-chain groups of the ATP γ C-bound state of PKA-C.

Residue	T_2 (ms)	S^2	Residue	T_2 (ms)	S^2
V15-C γ 1	8.52 ± 0.50	0.29 ± 0.02	I180-C δ 1	9.81 ± 0.35	0.25 ± 0.02
L19-C δ 2	4.73 ± 0.15	0.53 ± 0.02	V182-C γ 1	2.96 ± 0.40	0.85 ± 0.12
L27-C δ 1	4.39 ± 0.13	0.57 ± 0.02	V182-C γ 2	3.26 ± 0.18	0.77 ± 0.04
L27-C δ 2	4.54 ± 0.14	0.55 ± 0.02	V191-C γ 1	10.65 ± 0.56	0.24 ± 0.02
L40-C δ 2	4.27 ± 0.27	0.59 ± 0.04	V191-C γ 2	10.43 ± 0.65	0.24 ± 0.04
I46-C δ 1	9.01 ± 0.44	0.28 ± 0.01	L198-C δ 1	5.03 ± 0.48	0.50 ± 0.05
L59-C δ 1	4.61 ± 0.12	0.54 ± 0.01	L198-C δ 2	11.84 ± 0.55	0.21 ± 0.01
L59-C δ 2	4.28 ± 0.13	0.59 ± 0.02	L205-C δ 1	4.93 ± 0.15	0.51 ± 0.02
V60-C γ 1	2.38 ± 0.14	1.05 ± 0.06	I209-C δ 1	3.37 ± 0.09	0.74 ± 0.02
V60-C γ 2	4.54 ± 0.30	0.55 ± 0.04	I210-C δ 1	5.97 ± 0.13	0.42 ± 0.01
I73-C δ 1	5.34 ± 0.27	0.47 ± 0.02	L211-C δ 1	3.99 ± 0.17	0.63 ± 0.02
L74-C δ 1	7.62 ± 0.39	0.33 ± 0.02	L211-C δ 2	3.71 ± 0.07	0.68 ± 0.01
L74-C δ 2	15.06 ± 1.83	0.17 ± 0.02	V219-C γ 1	2.72 ± 0.16	0.92 ± 0.05
V79-C γ 2	3.77 ± 0.05	0.66 ± 0.01	V219-C γ 2	2.85 ± 0.14	0.88 ± 0.03
V80-C γ 1	3.59 ± 0.12	0.70 ± 0.02	L224-C δ 1	2.98 ± 0.12	0.84 ± 0.03
V80-C γ 2	3.76 ± 0.10	0.67 ± 0.02	L224-C δ 2	3.57 ± 0.09	0.70 ± 0.02
L82-C δ 1	3.13 ± 0.48	0.80 ± 0.13	V226-C γ 2	3.92 ± 0.20	0.64 ± 0.03
L82-C δ 2	3.72 ± 0.06	0.67 ± 0.01	L227-C δ 2	3.04 ± 0.07	0.77 ± 0.02
I85-C δ 1	3.82 ± 0.06	0.66 ± 0.01	I228-C δ 1	3.13 ± 0.05	0.80 ± 0.13
L89-C δ 1	3.93 ± 0.20	0.64 ± 0.03	I244-C δ 1	13.12 ± 0.42	0.19 ± 0.01
L89-C δ 2	4.38 ± 0.25	0.57 ± 0.03	I246-C δ 1	6.75 ± 0.47	0.37 ± 0.03
I94-C δ 1	4.07 ± 0.06	0.62 ± 0.01	V251-C γ 1	5.98 ± 0.11	0.42 ± 0.01
L95-C δ 2	4.38 ± 0.34	0.57 ± 0.04	V251-C γ 2	4.35 ± 0.16	0.58 ± 0.01
V98-C γ 1	3.49 ± 0.20	0.72 ± 0.04	V255-C γ 1	9.55 ± 0.45	0.26 ± 0.01
V98-C γ 2	2.95 ± 0.15	0.85 ± 0.04	V255-C γ 2	11.79 ± 0.43	0.21 ± 0.01
L103-C δ 1	4.42 ± 0.16	0.57 ± 0.02	L265-C δ 1	2.71 ± 0.14	0.93 ± 0.05
L103-C δ 2	4.69 ± 0.32	0.53 ± 0.04	L265-C δ 2	3.53 ± 0.20	0.71 ± 0.04
V104-C γ 1	3.91 ± 0.67	0.64 ± 0.11	L268-C δ 2	3.35 ± 0.15	0.75 ± 0.03
V104-C γ 2	4.41 ± 0.33	0.57 ± 0.04	L269-C δ 1	3.16 ± 0.15	0.79 ± 0.04
L106-C δ 2	4.98 ± 0.22	0.50 ± 0.02	L269-C δ 2	3.92 ± 0.12	0.64 ± 0.02
L116-C δ 1	3.55 ± 0.15	0.71 ± 0.03	L272-C δ 1	4.03 ± 0.12	0.62 ± 0.02
L116-C δ 2	3.03 ± 0.12	0.83 ± 0.03	L272-C δ 2	3.47 ± 0.13	0.72 ± 0.03
V119-C γ 1	3.33 ± 0.27	0.75 ± 0.06	L273-C δ 1	3.40 ± 0.12	0.74 ± 0.03
V119-C γ 2	3.24 ± 0.10	0.77 ± 0.02	L273-C δ 2	3.18 ± 0.07	0.79 ± 0.02
V123-C γ 1	2.43 ± 0.15	1.03 ± 0.07	V275-C γ 1	6.64 ± 0.16	0.38 ± 0.01
V123-C γ 2	4.47 ± 0.19	0.56 ± 0.02	V275-C γ 2	6.96 ± 0.12	0.36 ± 0.01
L132-C δ 1	3.84 ± 0.28	0.65 ± 0.05	L277-C δ 1	11.74 ± 0.11	0.21 ± 0.02
L132-C δ 2	3.39 ± 0.14	0.66 ± 0.02	L277-C δ 2	6.41 ± 0.28	0.39 ± 0.02

I135-C δ 1	3.64 ± 0.09	0.69 ± 0.02	L284-C δ 1	4.32 ± 0.11	0.58 ± 0.01
I150-C δ 1	8.45 ± 0.33	0.30 ± 0.01	L284-C δ 2	6.95 ± 0.19	0.59 ± 0.02
V151-C γ 1	3.27 ± 0.06	0.77 ± 0.01	V288-C γ 1	9.17 ± 0.77	0.27 ± 0.02
V151-C γ 2	3.13 ± 0.07	0.80 ± 0.02	V288-C γ 2	9.27 ± 0.37	0.27 ± 0.01
L152-C δ 1	3.46 ± 0.13	0.72 ± 0.03	I291-C δ 1	3.86 ± 0.09	0.37 ± 0.01
L152-C δ 2	3.39 ± 0.15	0.74 ± 0.03	I303-C δ 1	13.12 ± 0.59	0.20 ± 0.01
L157-C δ 1	4.22 ± 0.14	0.59 ± 0.02	I305-C δ 1	8.84 ± 0.25	0.28 ± 0.01
L160-C δ 1	3.12 ± 0.13	0.80 ± 0.03	V310-C γ 1	7.67 ± 0.37	0.33 ± 0.02
L160-C δ 2	4.42 ± 0.21	0.57 ± 0.03	I315-C δ 1	11.16 ± 0.76	0.22 ± 0.02
L162-C δ 2	3.25 ± 0.27	0.77 ± 0.06	I335-C δ 1	8.14 ± 0.21	0.31 ± 0.01
I163-C δ 1	3.36 ± 0.07	0.75 ± 0.02	V337-C γ 1	3.98 ± 0.11	0.63 ± 0.02
L167-C δ 1	3.49 ± 0.33	0.72 ± 0.07	V337-C γ 2	4.85 ± 0.07	0.51 ± 0.01
L167-C δ 2	3.66 ± 0.18	0.68 ± 0.03	I339-C δ 1	8.19 ± 0.24	0.31 ± 0.01
L172-C δ 2	7.44 ± 0.88	0.34 ± 0.04			
L173-C δ 1	5.24 ± 0.71	0.48 ± 0.07			
I174-C δ 1	7.29 ± 0.34	0.34 ± 0.16			

table S5. T_2 and S^2 values for methyl side-chain groups of the ATP γ N/PKI₅₋₂₄-bound state of PKA-C.

Residue	T_2 (ms)	S^2	Residue	T_2 (ms)	S^2
V15-C γ 1	8.75 ± 0.72	0.30 ± 0.02	L173-C δ 1	5.82 ± 0.31	0.45 ± 0.01
V15-C γ 1	6.76 ± 0.11	0.38 ± 0.01	L173-C δ 2	3.98 ± 0.33	0.65 ± 0.04
L19-C δ 2	4.74 ± 0.11	0.55 ± 0.01	I174-C δ 1	10.66 ± 0.31	0.24 ± 0.01
L27-C δ 1	4.71 ± 0.11	0.55 ± 0.01	I180-C δ 1	12.12 ± 0.52	0.21 ± 0.01
L27-C δ 2	4.55 ± 0.15	0.57 ± 0.02	V182-C γ 1	3.18 ± 0.22	0.82 ± 0.06
L40-C δ 2	3.79 ± 0.19	0.68 ± 0.4	V182-C γ 2	3.22 ± 0.15	0.81 ± 0.04
I46-C δ 1	8.92 ± 0.52	0.29 ± 0.02	V191-C γ 1	12.21 ± 0.56	0.21 ± 0.01
L49-C δ 1	3.63 ± 0.14	0.71 ± 0.02	V191-C γ 2	9.45 ± 0.37	0.27 ± 0.01
L49-C δ 2	3.19 ± 0.16	0.81 ± 0.04	L198-C δ 1	9.92 ± 0.56	0.26 ± 0.01
V57-C γ 1	3.49 ± 0.15	0.74 ± 0.03	L198-C δ 2	9.43 ± 0.61	0.28 ± 0.02
V57-C γ 2	4.24 ± 0.31	0.61 ± 0.05	L205-C δ 1	5.29 ± 0.26	0.49 ± 0.02
L59-C δ 1	3.55 ± 0.08	0.73 ± 0.02	L205-C δ 2	5.61 ± 0.38	0.46 ± 0.03
L59-C δ 2	3.56 ± 0.21	0.73 ± 0.04	I209-C δ 1	3.90 ± 0.21	0.67 ± 0.04
V60-C γ 1	2.78 ± 0.20	0.93 ± 0.07	I210-C δ 1	4.38 ± 0.12	0.59 ± 0.02
V60-C γ 2	3.46 ± 0.05	0.75 ± 0.01	L211-C δ 1	4.47 ± 0.17	0.58 ± 0.02
I73-C δ 1	5.64 ± 0.23	0.46 ± 0.02	L211-C δ 2	4.11 ± 0.09	0.63 ± 0.01
L74-C δ 1	5.40 ± 0.26	0.48 ± 0.02	V219-C γ 1	2.72 ± 0.09	0.95 ± 0.03
L74-C δ 2	5.40 ± 0.34	0.48 ± 0.03	V219-C γ 2	3.54 ± 0.15	0.73 ± 0.03
V79-C γ 2	3.20 ± 0.05	0.66 ± 0.01	L224-C δ 1	3.22 ± 0.02	0.81 ± 0.00
V80-C γ 1	3.68 ± 0.21	0.71 ± 0.04	L224-C δ 2	3.74 ± 0.09	0.69 ± 0.02
V80-C γ 2	5.43 ± 0.09	0.48 ± 0.01	V226-C γ 1	3.25 ± 0.10	0.80 ± 0.02
L82-C δ 1	3.34 ± 0.11	0.76 ± 0.02	V226-C γ 2	3.47 ± 0.09	0.75 ± 0.02
L82-C δ 2	4.55 ± 0.17	0.57 ± 0.02	L227-C δ 2	2.98 ± 0.07	0.87 ± 0.02
I85-C δ 1	3.79 ± 0.16	0.69 ± 0.03	I228-C δ 1	3.22 ± 0.12	0.81 ± 0.13
L89-C δ 1	4.54 ± 0.16	0.57 ± 0.02	I244-C δ 1	12.41 ± 0.62	0.21 ± 0.01
L89-C δ 2	5.02 ± 0.31	0.52 ± 0.03	I246-C δ 1	3.57 ± 0.12	0.73 ± 0.02
I94-C δ 1	3.65 ± 0.10	0.71 ± 0.02	I250-C δ 1	3.44 ± 0.19	0.75 ± 0.03
L95-C δ 1	6.57 ± 0.46	0.39 ± 0.03	V251-C γ 1	5.24 ± 0.12	0.50 ± 0.01
L95-C δ 2	4.71 ± 0.42	0.55 ± 0.05	V251-C γ 2	4.55 ± 0.24	0.57 ± 0.03
V98-C γ 1	3.86 ± 0.12	0.67 ± 0.02	V255-C γ 1	9.67 ± 0.83	0.27 ± 0.02
V98-C γ 2	3.30 ± 0.10	0.79 ± 0.02	V255-C γ 2	12.96 ± 0.41	0.20 ± 0.01
L103-C δ 1	3.75 ± 0.24	0.69 ± 0.05	L265-C δ 1	2.92 ± 0.13	0.89 ± 0.05
L103-C δ 2	4.60 ± 0.15	0.56 ± 0.02	L265-C δ 2	3.71 ± 0.11	0.70 ± 0.04
V104-C γ 1	5.34 ± 0.56	0.49 ± 0.05	L268-C δ 1	3.94 ± 0.17	0.66 ± 0.03
V104-C γ 2	4.37 ± 0.27	0.59 ± 0.04	L268-C δ 2	3.37 ± 0.16	0.77 ± 0.04
L106-C δ 1	4.96 ± 0.13	0.52 ± 0.01	L269-C δ 1	3.55 ± 0.17	0.73 ± 0.04
L106-C δ 2	5.23 ± 0.38	0.50 ± 0.04	L269-C δ 2	3.49 ± 0.12	0.74 ± 0.03
L116-C δ 1	4.10 ± 0.12	0.63 ± 0.02	L272-C δ 1	3.79 ± 0.15	0.68 ± 0.03
L116-C δ 2	3.68 ± 0.11	0.71 ± 0.02	L272-C δ 2	3.64 ± 0.11	0.72 ± 0.02

V119-C γ 1	3.58 ± 0.22	0.73 ± 0.04	L273-C δ 1	3.43 ± 0.09	0.76 ± 0.02
V119-C γ 2	3.37 ± 0.14	0.77 ± 0.03	L273-C δ 2	3.48 ± 0.09	0.75 ± 0.02
V123-C γ 1	2.79 ± 0.10	0.93 ± 0.03	V275-C γ 1	6.45 ± 0.18	0.40 ± 0.01
V123-C γ 2	3.45 ± 0.17	0.75 ± 0.04	V275-C γ 2	8.79 ± 0.47	0.30 ± 0.02
L132-C δ 1	3.47 ± 0.15	0.75 ± 0.03	L277-C δ 1	11.06 ± 0.31	0.23 ± 0.01
L132-C δ 2	3.67 ± 0.20	0.71 ± 0.04	L277-C δ 2	7.72 ± 0.19	0.34 ± 0.01
I135-C δ 1	6.18 ± 0.27	0.42 ± 0.02	L284-C δ 1	4.35 ± 0.12	0.60 ± 0.02
I150-C δ 1	5.95 ± 0.19	0.44 ± 0.01	L284-C δ 2	4.01 ± 0.14	0.65 ± 0.02
V151-C γ 1	3.19 ± 0.12	0.81 ± 0.03	V288-C γ 1	8.77 ± 0.42	0.30 ± 0.01
V151-C γ 2	3.35 ± 0.15	0.78 ± 0.03	V288-C γ 2	7.44 ± 0.36	0.35 ± 0.02
L152-C δ 1	3.55 ± 0.25	0.73 ± 0.05	I291-C δ 1	4.71 ± 0.18	0.55 ± 0.02
L152-C δ 2	3.67 ± 0.08	0.71 ± 0.02	I303-C δ 1	12.68 ± 0.69	0.20 ± 0.01
L157-C δ 1	3.06 ± 0.18	0.71 ± 0.02	I305-C δ 1	9.09 ± 0.37	0.29 ± 0.01
L160-C δ 1	3.60 ± 0.18	0.72 ± 0.02	V310-C γ 1	4.30 ± 0.12	0.60 ± 0.02
L160-C δ 2	4.38 ± 0.16	0.59 ± 0.04	I315-C δ 1	11.60 ± 0.83	0.20 ± 0.01
L162-C δ 1	3.72 ± 0.18	0.70 ± 0.04	I335-C δ 1	9.21 ± 0.19	0.28 ± 0.01
L162-C δ 2	3.32 ± 0.13	0.78 ± 0.03	V337-C γ 1	4.11 ± 0.13	0.63 ± 0.02
I163-C δ 1	3.57 ± 0.05	0.73 ± 0.01	V337-C γ 2	4.81 ± 0.17	0.54 ± 0.02
L167-C δ 1	3.56 ± 0.13	0.73 ± 0.03	I339-C δ 1	8.37 ± 0.33	0.31 ± 0.01
L167-C δ 2	3.16 ± 0.11	0.82 ± 0.03			
L172-C δ 1	3.62 ± 0.09	0.72 ± 0.02			
L172-C δ 2	3.16 ± 0.06	0.82 ± 0.02			

table S6. Group fits of CPMG dispersion curves measured at 700 and 850 MHz of the apo form of PKA-C.

Apo Group 1	R_{ex} (700 MHz, s⁻¹)	R_{ex} (850 MHz, s⁻¹)	Δω (ppm)	α	p_A (%)	k_{ex} (s⁻¹)
I150-Cδ1	26.3 ± 0.6	28.9 ± 1.3	0.94 ± 0.03	0.5 ± 0.1	94.4 ± 0.1	633 ± 70
L167-Cδ1	8.7 ± 0.8	11.7 ± 0.9	0.34 ± 0.02	1.5 ± 0.1		
L167-Cδ2	13.1 ± 0.7	16.7 ± 0.6	0.45 ± 0.02	1.2 ± 1.2		
L172-Cδ1	14.2 ± 0.5	17.8 ± 0.4	0.47 ± 0.01	1.2 ± 0.1		
L172-Cδ2	6.4 ± 0.8	8.9 ± 0.9	0.28 ± 0.02	1.6 ± 0.1		
I180-Cδ1	5.0 ± 0.7	7.0 ± 0.9	0.24 ± 0.02	1.7 ± 1.0		
L205-Cδ1	15.8 ± 0.7	19.5 ± 0.6	0.63 ± 0.02	1.1 ± 0.1		

Apo Group 2	R_{ex} (700 MHz, s⁻¹)	R_{ex} (850 MHz, s⁻¹)	Δω (ppm)	α	p_A (%)	k_{ex} (s⁻¹)
V57-Cγ1	16.9 ± 1.0	19.2 ± 1.7	0.51 ± 0.06	0.7 ± 0.3	4.5	426 ± 128
L162-Cδ2	12.7 ± 1.7	15.4 ± 1.6	0.53 ± 0.03	1.0 ± 0.3		
L103-Cδ2	19.8 ± 1.3	21.7 ± 2.6	0.65 ± 0.09	0.5 ± 0.3		
L59-Cδ2	7.1 ± 1.8	9.5 ± 2.1	0.25 ± 0.04	1.5 ± 0.2		

Apo Group 3	R_{ex} (700 MHz, s⁻¹)	R_{ex} (850 MHz, s⁻¹)	Δω (ppm)	α	p_A (%)	k_{ex} (s⁻¹)
V104-Cγ1	17.6 ± 0.4	20.5 ± 0.6	0.78 ± 0.04	0.8 ± 0.1	95.9 ± 0.3	750 ± 66
V104-Cγ2	21.6 ± 0.7	24 ± 0.7	1.02 ± 0.06	0.5 ± 0.1		
L95-Cδ2	28 ± 0.9	28.9 ± 1.0	1.99 ± 0.07	0.2 ± 0.0		

table S7. Group fits of the CPMG relaxation dispersion curves measured at 700 and 850 MHz of the ATP γ C form of PKA-C.

ATP γ C Group	R _{ex} (700 MHz, s ⁻¹)	R _{ex} (850 MHz, s ⁻¹)	$\Delta\omega$ (ppm)	α	p _A (%)	k _{ex} (s ⁻¹)
I150-C δ 1	13.0 ± 0.6	17.4 ± 0.9	1.22 ± 0.05	1.6 ± 0.1	97.7 ± 0.1	2500 ± 240
L172-C δ 1	11.1 ± 0.8	15.1 ± 1.0	1.12 ± 0.06	1.6 ± 0.1		
L173-C δ 1	7.9 ± 0.7	10.9 ± 1.0	0.91 ± 0.05	1.7 ± 0.0		
I174-C δ 1	8.7 ± 0.7	11.1 ± 0.9	0.92 ± 0.06	1.7 ± 0.0		
V104-C γ 1	15.8 ± 0.6	20.8 ± 0.8	1.40 ± 0.04	1.4 ± 0.1		
I180-C δ 1	9.8 ± 0.6	13.4 ± 0.8	1.03 ± 0.05	1.6 ± 0.1		
L95-C δ 1	12.5 ± 0.9	16.8 ± 1.2	1.20 ± 0.06	1.5 ± 0.1		
L95-C δ 2	10.5 ± 1.4	14.3 ± 0.5	1.08 ± 0.01	1.6 ± 0.1		
V182-C γ 2	7.0 ± 0.6	9.8 ± 0.8	0.85 ± 0.06	1.7 ± 0.0		
L103-C δ 2	2.7 ± 0.4	3.9 ± 0.9	0.51 ± 0.06	1.9 ± 0.0		
I94-C δ 1	7.0 ± 0.5	9.8 ± 0.7	0.85 ± 0.04	1.7 ± 0.0		
L162-C δ 2	6.9 ± 0.4	9.7 ± 0.5	0.85 ± 0.02	1.7 ± 0.0		

table S8. Single-quantum individual site fits of CPMG relaxation dispersion curves measured at 700 and 850 MHz of the apo form of PKA-C.

Apo	R _{ex} (700 MHz, s ⁻¹)	R _{ex} (850 MHz, s ⁻¹)	Δω (ppm)	α	p _A (%)	k _{ex} (s ⁻¹)	χ ²
L19-Cδ1	1.8 ± 0.7	2.6 ± 1.0	0.12±0.69	1.9 ± 0.8	78± 21	1670 ± 2380	13.5
L27-Cδ1	1.6 ± 0.7	2.4± 1.2	1.94± 0.56	0.3 ± 0.5	99.6± 7	920 ± 1820	8.08
L49-Cδ1	9.0 ± 1.2	13.4 ± 2.2	0.18± 0.26	0.6 ± 0.6	99.5± 9	2300 ± 3300	34.12
V57-Cγ1	18.0 ± 2.2	21.9 ± 4.8	0.43± 0.16	1.0 ± 0.7	92.4± 14	490± 210	4.35
L59-Cδ2	7.2 ± 1.3	9.3 ± 2.6	0.26± 0.15	1.3 ± 0.7	94.4± 20	400± 160	2.16
I73-Cδ1	2.2 ± 1.7	2.7 ± 1.9	0.39± 0.26	1.0 ± 0.8	98.9± 20	470± 360	68.00
L82-Cδ2	16.4 ± 0.7	20.1 ± 1.4	0.92± 0.15	1.1 ± 0.3	96.7± 4.8	1130± 270	33.41
I94-Cδ1	3.9 ± 0.3	5.8 ± 0.5	0.19± 0.38	2.0± 0.4	75.4± 20	2140± 550	14.74
L95-Cδ2	29.5 ± 0.4	5.4 ± 0.9	1.02± 0.54	1.4± 0.6	99.1± 20	930± 430	30.06
L103-Cδ2	19.7 ± 1.2	21.2 ± 2.0	0.66± 0.07	0.4± 024	93.6± 20	390± 140	7.32
V104-Cγ1	19.1 ± 0.8	22.8 ± 2.2	0.64± 0.08	0.9 ± 0.3	94.6± 1.5	680± 130	12.58
V104-Cγ2	20.7 ± 0.5	23.6 ± 1.0	1.01± 0.06	0.7± 0.2	96.5± 0.02	980± 160	6.11
I150-Cδ2	26.2 ± 0.4	28.6 ± 0.8	0.94± 0.00	0.5 ± 0.1	94.3± 0.001	620± 45	3.46
L157-Cδ1	3.9 ± 0.4	4.6 ± 0.8	1.18± 0.38	0.8 ± 0.6	99.4± 9.1	1170± 760	12.56
L160-Cδ2	18.4 ± 0.8	26.2 ± 1.6	0.30 ± 0.09	1.8 ± 0.4	84± 17	710± 100	2.51
L162-Cδ1	12.3 ± 1.5	14.1 ± 3.0	0.43± 0.17	0.7± 0.7	94.6± 16	360± 220	12.2
I163-Cδ1	4.5 ± 0.6	6.6 ± 1.2	0.09± 0.17	1.9± 0.7	50.0± 21	540± 160	14.37
L167-Cδ1	7.8 ± 0.4	9.3 ± 0.7	0.86± 0.22	0.9± 0.5	98.3± 9.5	950± 370	13.86
L167-Cδ2	13.0 ± 1.2	14.4 ± 2.1	0.58± 0.17	1.2 ± 0.3	95.6± 12	420± 270	18.67
L172-Cδ1	13.9 ± 0.7	16.4 ± 1.7	0.55± 0.09	0.8± 0.4	95.3± 6.6	540± 150	30.00
L172-Cδ2	9.2 ± 8.2	13.9 ± 12.1	0.11± 0.18	2.1 ± 0.9	50.0± 19.7	420± 180	22.67
I174-Cδ1	4.1± 0.4	5.4± 0.8	0.65± 0.36	1.4 ± 0.7	98.7± 16.7	1200± 570	30.67
I180-Cδ1	5.4± 0.7	8.1± 1.4	0.10± 0.12	2.1 ± 0.5	50.0± 21.2	590± 120	54.59
V191-Cγ1	2.2± 0.6	2.7± 0.9	1.53± 0.64	1.1 ± 0.5	99.7± 7.3	1780± 1400	10.06
L198-Cδ1	3.7± 2.6	3.7± 3.1	2.97± 1.01	0.0 ± 0.3	99.4± 5.4	610± 1800	8.67
L205-Cδ1	18.2± 1.3	19.8± 2.6	0.50± 0.12	0.4 ± 0.4	92.5± 12.1	320± 170	7.45
L227-Cδ1	2.0± 0.8	2.0± 0.8	0.11± 0.33	2.0 ± 0.8	50.0± 21.1	990± 420	5.12
V288-Cγ1	2.2± 0.2	2.5± 0.4	0.85± 0.34	0.6 ± 0.7	99.5± 15.3	720± 460	10.79
I291-Cδ1	5.4± 0.9	6.0± 1.7	0.37± 0.14	0.5 ± 0.6	97.0± 10.6	270± 140	5.79
I303-Cδ1	2.3± 1.0	3.4± 1.3	0.39± 0.92	2.0 ± 0.6	95.4± 19.3	3310± 2000	78.03
V310-Cγ1	1.6± 0.2	2.4± 0.3	0.15± 0.53	2.1 ± 0.5	83.3± 21.8	2240± 710	37.29

table S9. Individual fits of the CPMG dispersion curves measured at 700 and 850 MHz of the ATP γ C-bound state of PKA-C.

ATP γ C	R _{ex} (700 MHz, s ⁻¹)	R _{ex} (850 MHz, s ⁻¹)	Δω (ppm)	α	p _A (%)	k _{ex} (s ⁻¹)	χ ²
L19-Cδ2	1.8 ± 1.5	2.7 ± 2.0	0.15±1.80	2.0 ± 0.1	66± 22	3400 ± 3600	6.45
L40-Cδ2	2.8 ± 0.7	2.9± 1.2	1.94± 0.56	0.3 ± 0.5	99.6± 7	920 ± 1820	8.08
V80-C γ 1	8.5 ± 6.3	9.5 ± 7.5	3.00± 1.58	0.6 ± 0.6	99.5± 9	2300 ± 3300	34.12
I85-Cδ1	3.8 ± 1.9	4.3 ± 2.6	1.50± 0.86	0.6 ± 0.7	99.5± 9	1270± 2100	55.13
I94-Cδ1	7.6 ± 3.0	10.6 ± 4.4	1.50± 0.86	1.7 ± 0.4	98.4± 16	3750± 2540	41.91
L95-Cδ1	12.2 ± 0.7	15.5 ± 1.4	1.30± 0.84	1.3 ± 0.3	98.4± 1.3	2210± 570	11.61
L95-Cδ2	17.0 ± 4.4	24.1 ± 6.4	1.44± 0.19	1.8 ± 0.4	96± 20	3900± 1590	3.24
V98-Cδ2	3.8 ± 0.4	4.4 ± 0.7	0.97± 0.28	0.7± 0.6	99.3± 7.5	860± 660	3.28
L103-Cδ2	4.1 ± 0.4	5.4 ± 0.9	1.02± 0.54	1.4± 0.6	99.1± 20	1940± 850	14.21
V104-C γ 1	3.8 ± 0.4	4.4 ± 0.7	1.34± 0.61	1.6± 0.4	96.8± 20	3200± 2040	14.29
V104-C γ 2	3.8 ± 0.4	4.4 ± 0.7	0.14± 0.76	2.0 ± 0.7	78± 21	1990± 2510	9.17
L132-Cδ1	3.4 ± 1.1	5.0 ± 1.7	0.16± 0.57	2.0± 0.8	76.5± 20	1690± 1530	23.94
I150-Cδ1	13.2 ± 0.8	18.2 ± 1.7	1.18± 0.42	1.6 ± 0.3	97.2± 14	2890± 620	53.87
L160-Cδ2	9.4 ± 6.3	13.9 ± 8.7	0.51± 1.62	2.0± 0.4	75.7± 21	6200± 4150	14.31
L162-Cδ2	5.2 ± 0.6	7.7 ± 1.2	0.25± 0.55	2.0 ± 0.5	74± 21	2710± 1100	3.55
L167-Cδ1	4.2 ± 0.4	4.7 ± 0.7	1.44± 0.30	0.6± 0.5	99.4± 7	990± 680	6.3
L172-Cδ1	10.7 ± 0.8	12.6 ± 1.6	1.28± 0.27	0.8 ± 0.3	98.5± 7	1300± 620	27.45
L173-Cδ1	10.7 ± 6.8	13.9 ± 8.5	2.05± 1.51	2.0± 0.4	98.9± 16	3550± 2900	37.31
I174-Cδ1	8.7 ± 0.4	11.1 ± 0.9	1.49± 0.24	1.2 ± 0.3	98.9± 4	2200± 570	28.03
I180-Cδ1	10.0 ± 0.8	14.3 ± 1.6	0.80± 0.44	1.8± 0.3	95.6± 15	3060± 800	216.26
V182-C γ 2	7.9 ± 0.5	9.2 ± 1.1	1.62± 0.22	0.8 ± 0.4	99.1± 1.3	1560± 750	55.98
V191-C γ 1	2.2± 0.2	2.2± 0.2	2.38± 0.15	0.0 ± 0.0	91.7± 1.7	24.7± 25.3	22.39
L272-Cδ1	3.0± 0.9	3.0± 1.2	2.07± 0.62	0 ± 0.4	99.7± 7.1	350± 1100	10.34
L284-Cδ2	2.2± 0.2	4.3± 0.5	0.16± 0.44	2.0 ± 0.4	71.7± 21	2200± 620	16.21
V310-C γ 1	3.4± 0.2	4.7± 0.3	0.71± 0.37	1.7 ± 0.5	98.9± 14	1640± 460	18.45

table S10. Single-quantum individual site fits of CPMG curves at 700 and 850 MHz of the ATP γ N/PKI₅₋₂₄-bound state of PKA-C.

ATP γ N/PKI ₅₋₂₄	R _{ex} (700 MHz, s ⁻¹)	R _{ex} (850 MHz, s ⁻¹)	Δω (ppm)	α	p _A (%)	k _{ex} (s ⁻¹)	χ ²
V15-C γ 1	5.9 ± 0.4	8.7 ± 0.6	0.24±0.36	2.0 ± 0.2	50± 21	2900 ± 500	9.07
L19-Cδ2	2.5 ± 2.1	3.7 ± 2.8	0.17±1.50	2.0 ± 0.5	50± 21.5	3400 ± 3700	5.95
I303-Cδ1	7.6 ± 1.8	11.2 ± 2.5	0.58	2.0 ± 0.2	50± 19	4050 ± 1200	261.50

table S11. Approximate R_{ex} values from two points of the CPMG experiment for the ATP γ N/PLN₁₋₁₉-bound form of PKA-C.

Residue	R_{ex} (s ⁻¹)	Residue	R_{ex} (s ⁻¹)	Residue	R_{ex} (s ⁻¹)	Residue	R_{ex} (s ⁻¹)
V15-C γ 1	0.57±0.18	L103-C δ 1	6.73±0.66	L172-C δ 2	9.88±1.47	L265-C δ 1	0.53±0.73
V15-C γ 2	5.05±0.13	L103-C δ 2	3.05±0.63	L173-C δ 1	12.22±0.41	L265-C δ 2	1.29±0.81
L19-C δ 2	3.16±0.12	V104-C γ 1	15.97±0.31	L173-C δ 2	3.53±0.95	L268-C δ 1	-0.47±0.43
L27-C δ 1	0.24±0.37	V104-C γ 2	1.50±1.00	I174-C δ 1	18.86±0.16	L268-C δ 2	-0.29±0.21
L27-C δ 2	16±0.43	L106-C δ 1	1.60±0.31	I180-C δ 1	14.25±0.16	L269-C δ 1	-2.48±1.19
L40-C δ 1	8.90±0.14	L106-C δ 2	1.87±0.36	V182-C γ 1	1.35±1.30	L269-C δ 2	0.52±0.33
L40-C δ 2	0.66±0.71	L116-C δ 1	6.66±0.51	V182-C γ 2	-0.39±0.12	L272-C δ 1	1.08±0.57
I46-C δ 1	5.60±0.03	L116-C δ 2	5.30±0.49	V191-C γ 1	10.40±0.10	L272-C δ 2	0.13±0.85
L49-C δ 1	16.21±1.29	V119-C γ 1	2.14±0.57	V191-C γ 2	1.47±0.13	L273-C δ 1	1.38±0.42
L49-C δ 2	16.60±1.16	V119-C γ 2	4.29±0.90	L198-C δ 1	24.77±0.53	L273-C δ 2	2.78±0.24
V57-C γ 2	3.93±0.87	V123-C γ 1	1.56±0.55	L198-C δ 2	8.66±0.08	V275-C γ 1	-0.05±0.22
L59-C δ 1	14.58±1.02	V123-C γ 2	7.36±1.73	L205-C δ 1	2.78±0.24	V275-C γ 2	3.14±0.10
L59-C δ 2	3.54±0.33	L132-C δ 1	3.54±0.33	I209-C δ 1	2.75±1.66	L277-C δ 1	-0.23±0.07
V60-C γ 1	-1.18±1.16	L132-C δ 2	17.90±0.1.27	I210-C δ 1	0.80±0.34	L284-C δ 1	-0.03±0.20
V60-C γ 2	0.25±0.33	I135-C δ 1	1.01±0.19	L211-C δ 1	-0.29±0.13	L284-C δ 2	1.08±0.57
I73-C δ 1	3.26±0.21	I150-C δ 1	10.35±0.56	L211-C δ 2	0.63±0.17	V288-C γ 1	12.40±0.37
L74-C δ 1	15.70±0.22	V151-C γ 1	0.24±0.36	V219-C γ 1	3.10±0.43	V288-C γ 2	3.73±0.036
L74-C δ 2	12.96±0.66	V151-C γ 2	0.33±0.37	L224-C δ 1	0.45±0.37	I291-C δ 1	1.28±0.11
V80-C δ 1	0.33±0.37	L152-C δ 1	1.60±0.57	L224-C δ 2	0.81±0.95	I303-C δ 1	7.43±0.02
V80-C δ 2	4.03±0.36	L152-C δ 2	0.38±0.25	V226-C γ 1	13.34±1.74	I305-C δ 1	2.45±0.11
L82-C δ 1	1.13±0.80	L157-C δ 1	22.86±2.01	V226-C γ 2	1.47±0.36	V310-C γ 1	8.60±0.22
L82-C δ 2	-0.46±0.43	L160-C δ 1	5.38±1.07	L227-C δ 2	7.13±0.62	I315-C δ 1	3.07±0.12
I85-C δ 1	5.25±0.73	L160-C δ 2	20.96±0.96	I228-C δ 1	-1.19±0.27	I335-C δ 1	16.40±0.22
L89-Cd1	0.22±0.96	L162-C δ 1	20.55±0.23	I244-C δ 1	2.07±0.06	V337-C γ 1	-0.37±0.12
L89-Cd2	11.08±0.64	L162-C δ 2	5.61±0.58	I250-C δ 1	5.55±1.06	V337-C γ 2	0.57±0.18
I94-C δ 1	20.75±0.91	I163-C δ 1	0.44±0.94	V251-C γ 1	0.57±0.18	I339-C δ 1	-0.82±0.13
L95-C δ 1	23.80±0.92	L167-C δ 1	5.22±0.84	V251-C γ 2	4.50±0.92		
V98-C γ 1	7.25±1.32	L167-C δ 2	2.47±0.95	V255-C γ 1	1.49±0.18		
V98-C γ 2	10.47±1.22	L172-C δ 1	13.26±0.45	V255-C γ 2	5.19±0.08		